University of Stavanger

Faculty of Science and Technology

MASTER'S THESIS

Study program/ Specialization: Petroleum Engineering – Master of Science Degree Programme	Spring semester, 2013 Open access
Writer: Kristine Geitle	…… (Writer's signature)
Faculty supervisor: Merete V. Madland	
Title of thesis: *Chemically induced compaction in fractured and intact chalk cores*	
Credits (ECTS):30	
Key words: • Chalk • Mons – Obourg Saint Vaast • Water weakening • SSW • $MgCl_2$ • Fractures • SEM images • Compaction	Pages: 78 + enclosure: N/A Stavanger, 16.06.2013 Date/year

Front page for master thesis
Faculty of Science and Technology
Decision made by the Dean October 30th 2009

Acknowledgements

First of all I want to express my deepest gratitude towards Ph.D. Reidar Inge Korsnes who was a skillful, encouraging and supportive supervisor throughout the whole process of writing this master thesis. I would also like to thank my faculty supervisor Associate Professor Merete Madla Vadland for the opportunity to participate in this exciting research programme, and for her excellent support and helpful feedback. In addition I would like to thank Tania Hildebrand -Habel and Mona Minde for providing me with SEM images concerning my experiments.

Also, special thanks to (Abubeker, 2013) for inspiring cooperation during this process and helpful guidance during experimental work to the very end of completing the thesis.

Finally, I would like to thank my family for the love and support, always believing in me and their encouragement during hard times – I could not have done this without them.

Thanks to all!

Kristine Geitle, Stavanger 16.06.2013

Abstract

The effect of pore water chemistry on the mechanical strength of chalk has been thoroughly investigated during the last years. Recent studies have demonstrated precipitation of new minerals that further triggers dissolution and increased deformation of chalk matrix when exposed to certain brines at reservoir temperatures. However, to detect these newly formed minerals and further localize the areas of precipitation by analyzing SEM (scanning electron microscopy) images, have proved to be a time-consuming and complicated process.

Until now, most research have been carried out on intact chalk cores while only minor attention have been devoted to study fractured cores. In this thesis, high porosity outcrop chalk from Mons was tested experimentally in triaxial cells - both fractured and intact. The temperature was kept at a constant value of 130°C (similar to reservoir conditions) and the cores were flooded with different types of brines; either synthetic seawater (SSW) or magnesium chloride (0.219M $MgCl_2$). Two mechanical tests were conducted; hydrostatic and creep, and effluent water was collected during this whole testing period. By analyzing the amount of ions present in the effluent made it possible to confirm if the injected brine was diffusing into the matrix, and not only through the fracture itself. SEM images would further support the overall observations provided from the experimental results.

The experimental work showed that the fractures did not have any remarkable effect on the mechanical strength during hydrostatic loading, were all cores were flooded with 0.657M NaCl. The small differences that occurred however, are most likely caused by variations in porosity values rather than the fractures. Also during the first 6 days of creep, it was continued to flood with 0.657M NaCl and all the cores witnessed of relatively similar behaviors, with a reduction in strain rate and further development of transient creep phase. When the flooding brines were substituted, more distinct observations could be seen. The cores flooded with SSW experienced the highest deformation rates despite that one core contained a fracture whereas the other one was intact, but the latter had a somewhat higher value when comparing the two. Similar behaviors were observed for the cores flooded with 0.219M $MgCl_2$, as the intact core had a slightly higher deformation rate. The reason for the increased deformation rate observed for the intact cores, was suggested to be a result of the core matrix being immediately contacted by the flooding fluid. For the cores containing fractures, the brine would spend longer time to diffuse into the matrix and hence deform the chalk core.

Chemical analysis of the effluent water have shown that magnesium is lost within the core in addition to calcium production, both for the fractured and intact cores when flooded with SSW and 0.219M $MgCl_2$. SEM images from one of the fractured cores also detected clay like minerals in the hole's wall and it was clear that the grain structure had been altered. Images from further out in the core exterior on the other hand, had cleaner grain surface as it was possible to see the coccolith rings.

Innhold

1 Introduction

Carbonate reservoirs can be classified as either limestone, dolomite (dolostone) and chalk. A substantial amount of the worlds hydrocarbons are trapped in carbonate reservoirs, and the number is believed to exceed as much as 50%. Yet, because of the complexities of carbonate rocks like low permeability, fractures, low water wetness and the rock being rather inhomogeneous, the average oil recovery is below 30% (Sheng, 2010). Chalk is a fine-grained limestone composed of coccolith skeletons that originates from planktonic algae and coarser debris such as calcite grains and shells. When chalk is buried at depths of approximately 1000 meters, diagenesis will normally cause a reduction of the porosity. However, for the chalk reservoirs located in the North Sea at 2000 to 3000 meters depth, porosities are exceptionally high ranging from 30% to even above 40%. There are three factors that contribute to prevent burial diagenesis and subsequent porosity reduction; a generated pressure that supports the overburden and in this way reduces the pressure solution, oil or gas occupied in the pore space and magnesium ions present in the pore water and seawater, thus retarding the diagenesis process. Even though the porosity is relatively high, the permeability of the chalks is only 1-3 milliDarcy (Hardman, 1982).

The Ekofisk field is a giant oil field located in the central graben on the Norwegian sector, and it was first discovered back in 1969. The field is developed in the naturally fractured chalk rocks from the geological periods of Upper Cretaceous to Lower Tertiary, having a reservoir depth of around 2900 meters and a temperature of approximately 130°C (Moore, 1989). When the Ekofisk field started production in 1971 by pressure depletion alone, the reservoir experienced compaction and sea-floor subsidence, which in turn accounted for 40% of the drive mechanism. After pressure depletion declined, water injection was introduced in 1987 to enhance the oil recovery and create a pressure support to prevent further compaction of the reservoir. Seawater injection turned out to be very successful as the oil recovery is evaluated to be close to 50% (Sheng, 2010). However, the compaction still continued despite that the reservoir had regained its initial pressure. It seemed like the sea water reacted with chalk at high temperatures and thus affected the mechanical properties of the rock. This phenomenon of chalk-water interaction is usually referred to as *water weakening of chalk* (Madland et al., 2011).

Although this water weakening phenomenon has a positive effect on oil recovery due to compaction, it has also given the oil companies some great expenses. One of the negative consequences of reservoir compaction and hence induced stresses in the formation is that the sea-floor can eventually start to give in and subside. This is what happened to the Ekofisk field in the early 80's after years of production. Several platforms had sunk approximately 2.5 meters compared to when they first got installed, and the discovery led to an extensive operation during the summer of 1987. Hydraulic jacks were used to lift the platforms almost

6.5 meters, making it a costly and challenging project (Kvendseth, 1988). Unstable wells, casing deformations and difficulties in well completion is other problems caused by sea-floor subsidence, as the compressional and tensional strains affects the formation (Nagel, 2001). Concerns like this makes the oil companies eager to find a solution behind the mystery of the water weakening phenomenon.

In the previous years scientists believed that the mechanical strength of chalk mainly was governed by the porosity and silica content alone (DaSilva, 1985). Most of the research was devoted to look upon the physical effects, while there was added little emphasis on the chemical effects. First in the early 1990's, water weakening was considered as being the main mechanism and extensive research has been going on since (Sylte, Thomas, Rhett, Bruning, & Nagel, 1999). In the following years there have been various attempts to explain how the rock is affected mechanically by the pore fluid, and the mechanisms behind this water weakening effect. The mechanisms are often classified as either capillary effects, chemical effects and physico-chemical effects and has been described by (Gutierrez, Høeg, & Øino, 2000):

Capillary forces are one of this water weakening mechanisms that has been granted much attention through the previous years. Capillary forces occur just at the interface between grain surfaces, when the rock is exposed to a pore fluid. This interaction will in turn create a surface tension if the chalk rock is contacted by either water (wetting fluid), oil or gas (non-wetting fluids). Even after the chalk is dried, there will still be some water left in the small pores from its original state. The remaining water will induce a contact pressure between the grains, as it pulls the grains together by cohesive forces, resulting in a strengthening effect of the chalk rock. However, if more water is introduced and fill up the voids - this force will disappear and have a opposite effect - thus making the rock weaker. Oil on the other hand, will not have an impact on the capillary force as it is a non-wetting fluid. Experiments performed by (Risnes & Flaageng, 1999) showed that mechanisms other than the capillary effects, also had to influence the weakening of chalk. The authors first saturated a core with methanol which is water-miscible and observed that the capillary forces disappeared as estimated. However, this core appeared to be mechanically stronger compared to the core flooded by water alone. This observation demonstrated that chalk strength also depends on the type of pore fluid, not only the capillary effect itself.

Physico-chemical effects occur when a fluid reacts with chalk, and thereby evokes a chemical reaction often referred to as stress-corrosion. This happens just at the crack tips as strong chemical bonds are gradually substituted with weaker bonds. When the strength is reduced in this manner, the cracks become more susceptible to stress, i.e. the tolerance level for the crack to propagate is much less. However, both the capillary effects and physico-chemical effects did not seem to affect the weakening of chalk in the extent that was being observed.

Chemical effects have been granted more attention through the last years, and processes such as precipitation, dissolution, substitution and intergranular pressure solution have been

suggested as possible water weakening factors (Reidar, Merete, Tor, Stig, & Geir). A dissolution process tends to occur when certain minerals are exposed to liquids and cause them to break up their bondings. Chalk which consists of calcium carbonate ($CaCO_3$) dissolves into Ca^{2+} and CO_3^{2-} ions as water is introduced, which in turn can result in the grain size becoming smaller and reduce the overall mass. This causes a decreased strength of the contact pressure created by the capillary forces, and hence contributes to weaken the chalk. In addition, (Butenuth & De Freitas, 1989) showed that when calcite reacts with an aqueous fluid, the crystal can experience alterations of the surface characteristics. Other experiments that were performed also showed that the solid surface area could undergo changes when exposed to an aqueous solution. Precipitation of minerals is another process that seems to occur when chalk gets in contact with water. This process on the other hand, might increase the rock strength as large minerals occupies the pores and tends to clog and cement the pore throats. (Reidar et al.) proposed a substitution process involving chalk exposed to seawater like brines at high temperatures. It appeared that magnesium ions (Mg^{2+}) dissolved in aqueous solution was capable to substitute calcium ions (Ca^{2+}) at the grain surface, and that the substitution process would increase with elevated temperatures. It was also suggested that the reaction required the presence of sulfate (SO_4^{2-}) in the pore fluid. However, more recent studies performed by (Madland et al., 2011) demonstrated that chalk cores flooded with only $MgCl_2$ experienced a substantial chemical deformation. It appeared that a comparable deformation would occur without any sulfate present in the fluid.

Extensive research programs have been funded and carried out through the years in an attempt to reveal the main mechanisms behind the water weakening effect. However, chalk-water interaction is proven to be a rather complicated process and the phenomenon of water weakening is still not fully understood.

The main objective of this thesis was to study how the mechanical strength of fractured and intact chalk cores was affected when exposed to different types of brines at a temperature of 130°C - similar to reservoir conditions. One factor that was of particular interest for the fractured core samples was to observe if the injected brine would interact with the chalk matrix, or more or less flow straight through the hole. By analyzing SEM (scanning electron microscopy) images of the core, it was possible to detect where to look for new minerals that we expected to form dominantly in the fracture region. In this way it will be easier in the future to quantify and localize these secondary minerals, and not look for “the needle in the haystack”. However, previous studies have shown that detection of these secondary minerals are a highly time consuming and complicated process.

The experiments were performed in co-operation with another master student (Abubeker, 2013), and all of the results are compared and presented in this thesis. Two different types of mechanical tests were carried out; hydrostatic and creep, followed by chemical analysis. The experiments were carried out in parallel, one core being fractured whereas the other one was intact. To compare how the mechanical strength of chalk was affected by the

presence of a fracture, two different flooding brines were used; synthetic seawater (SSW) and magnesium chloride ($MgCl_2$). By collecting effluent water during the creep phase, it was possible to analyze any potential losses or production of ions from the chalk core. The experimental results were then combined and interpreted to see if there was any water weakening effect on the chalk cores.

2 Theory

2.1 Carbonates

2.1.1 Carbonate rocks in general

Carbonate rocks are classified as a type of sedimentary rocks which primarily consists of carbonate minerals. Sedimentary rocks are deposited either as biogenic sediments, chemical precipitates or as clastic sediments (Bradl, 2005). The term clastic is derived from *klastos*, which is the Greek word for broken. Clastic sediments are made of eroded and weathered particles from other pre-existing rocks, and the size of the clast itself is a good indicator to distinguish between the different types of sedimentary rocks. Chemical precipitates on the other hand "has moved as dissolved chemical in solution. When the solution becomes too full of the chemicals, they precipitate as chemical sedimentary material". This occurs in seawater when a certain amount of water is lost as a consequence of evaporation, causing some of the salt crystals to cluster and form different minerals. In addition, sediments can be formed by chemical reactions triggered by plants or animals that exist in the water. Biogenic sediments are made of deposits from dead plants and animals, and the rocks can be classified as either bioclastic or organic. Bioclastic rocks contain parts of deceased living beings such as skeletons, while the organic rocks contain trapped carbon and hydrogen. When the organic compounds then are unable to decompose properly, they will eventually be turned into fossil fuels (Lawton, 1997). Because carbonate sediments can be deposited quite differently, the sediments are often found to have mixed particles with a variety of sizes, shapes and mineralogy. The variation among the particles can create voids in the carbonates, and hence give a high porosity. (Lucia, 1999)

2.1.2 Chalk

Chalk is a sedimentary rock and consists of over 90% calcium carbonate ($CaCO_3$). Pure chalks comprise of whole and fragmentary parts of calcite skeletal remains that originates from planktonic algae. These skeletons are built up of platelets or calcite tablets and usually have a dimension of around 1 µm. The calcite grains form ring-structures called coccoliths and are typically 10 µm in diameter. Pure chalks with high porosity often have an open structure and the dimensions of the pore space can be much larger than the grain size itself. This structure is caused by chalk having a mixture of coccolith rings which are intact as well as large and small fragments. The porosity can exceed 40%, but the permeability is rather small (1-3 milliDarcy). This is caused by the pore throats being very narrow due to the smallness of the grains (Risnes, 2001).

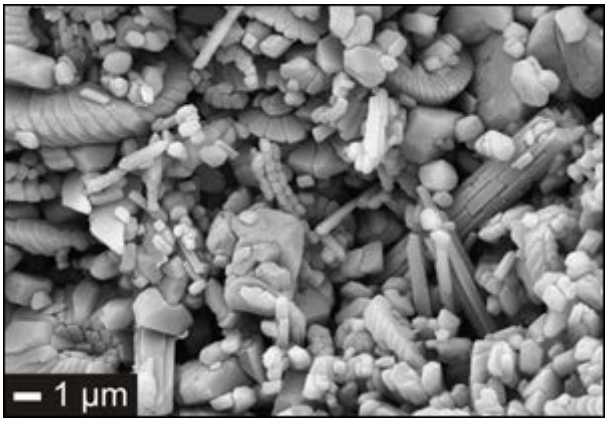

Figure 2.1: SEM image of Mons outcrop chalk (Tania Hildebrand – Habel, in-house data)

2.1.3 Chalk reservoirs

Despite the fact that Central Graben chalk reservoirs in the North Sea are located at several thousand meters depth, they still have exceptionally high porosities. With a few notable exceptions, the porosity (and permeability) of chalks decreases as a direct function of burial depth, hence making it rather unique (Scholle, 1977). The exceptions are an effect of overpressure, as well as the combination of fracturing, the timing of hydrocarbon generation, diagenesis, migration and entrapment (Fleet, Boldy, & Burley, 1999).

The porosity of chalks can be reduced through early seafloor cementation or by later burial diagenesis. This degree of cementation is related to burial depths, but it can vary as an effect of the chemistry of pore-water. If there is a presence of fluids in the pores containing small amounts of magnesium, this will in turn slow down cement generation. The porosity reduction of chalk caused by compaction are both mechanical and chemical, hence the effect of these can be retarded through overpressure. Differential stresses within chalks will then be reduced, and primary porosity can in this way be preserved. Another way which also contributes to maintaining the porosity is oil entering the rock in an early stage, resulting in exclusion of water. If chalks are located in depths of more than 2000 meters, it can act as an impermeable cap rock and trap the oil (Scholle, 1977).

Fractures in chalk reservoirs are of critical importance and for a reservoir to be productive, it needs these fractures to fill and drain the pore volumes. It contributes to increase the permeability of the formation and forms a path for petroleum production (Fleet et al., 1999). Chalks are in general severely fractured, but the distribution and geometry of the fractures can vary to a great extent. Understanding how these fractures are distributed and what controls the geometry, is therefore essential to be able to anticipate how the fluids will flow through the reservoir (Michael J.Welch, 2013).

The quality of a reservoir consisting of chalk is governed by several different conditions, but four factors dominate. These coccoliths mentioned earlier formed by calcite grains, are one important factor; how they are distributed during deposition as well as their size. The purity

of chalk in terms of calcium carbonate of the sediment, how quickly it is deposited and the way the reservoir is structured by tectonics also matters. For chalk to become a reservoir rock it needs to have low clay content and this is also the factor of greatest importance. In general, rocks with a maximum of 5% clay minerals are likely to form good reservoirs, between 5% and 10% fair reservoirs and if higher than 10 % the quality gets rather poor. So, with lower amounts of clay the more favorable the reservoir will be. Sea level changes are found to be closely correlated with the degree of clay accumulation in chalks (Hardman, 1982).

2.2 The Ekofisk field

The Ekofisk field is located within the Central Graben in the southern part of the North Sea, and has a reservoir depth of around 2900 meters. Because of an impermeable layer the chalk formation is divided in two separate parts; one called Ekofisk while the other is named Tor. Since the Ekofisk field started producing back in 1971, it has experienced a significant subsidence of the sea-floor. This phenomenon occurs when the oil gets extracted from the formation, which in turn reduces the overall pressure within the reservoir and cause compaction of the chalk (I.Trifu, 2002)

Workers at the Ekofisk installations had been talking about the fact that the platforms seemed to lay somewhat deeper in the water than before, but no one had investigated if it actually was the case. Late in the autumn of 1984, people began to make measurements on the installations and compared photographs taken early in the 1970's with new ones. The evidence confirmed the suspicion about sea-floor subsidence, and it turned out that the platforms were approximately 2,5 meters deeper in the water compared to when they first got installed.

Subsidence of the formation due to oil, gas and water extraction is a known phenomenon. As liquid and gas are removed from the reservoir rock initial pressure decreases, thus the formation above creates overburden on the carrier beds. Chalk is a relatively soft material compared to for example sandstone, which is most prevalent in Norway for oil and gas production. When the pressure then is reduced – and the soft chalk no longer can withstand the immense load – it will eventually give in and be compacted.

The Ekofisk field had in a short time been a major source of income, so it was crucial to find a solution to ensure future production. Various alternatives were proposed, but they were either too expensive to implement, the effect was fairly uncertain and some implies that the platforms had to shut down for an extended period. One suggestion remained; to elevate the platform decks. Several computer models had been constructed to calculate and simulate to which extent the sea-floor was subsiding. To know also how much the decks needed to be jacked up, it was necessary to predict what the total subsidence would be. Each of the models estimated the subsidence as a direct cause of compaction, and came up

with the same conclusion of around 6 meters. So during the summer of 1987, the platforms were lifted almost 6.5 meters by the use of hydraulic jacks (Kvendseth, 1988).

It was believed that the rate of subsidence eventually would decline, but it turned out that was not the case. The field continued this gradual compression and a new solution was finally introduced in 1987; water injection. As the oil gradually was removed from the reservoir, water would substitute for the oil and hence act as pressure support in the formation. In this way the effective stresses remained the same, and based on the laws of rock mechanics; if the stresses do not increase, further subsidence should be prevented. Also this prediction turned out to fail, and the formation continued to sink. Apparently, other factors affected the subsidence besides the effective stresses. Scientists then started to look at the chemical reactions that occur between water and chalk, when water is injected into the reservoir. This would prove to form a new expression called "water weakening"(Bjorlykke, 2010).

2.3 Mechanical properties – rock mechanics

The following theory and figures are based on the book "petroleum related rock mechanics" (Fjær, Holt, Horsrud, Raaen, & Risnes, 2008)

2.3.1 Elasticity

Elasticity is defined as a material's ability to resist some degree of deformation caused by forces, and also recovering from this deformation afterwards. Rock mechanics are based on this concept of elasticity, and it is essential within all aspects. When a material is exposed to a certain force, it often responds in a linear trend. That is, the external forces and the corresponding deformations have a linear relation. This applies to relatively small changes in the forces, and then the response is almost always linear. Deformation of a rock material can also change with time when external conditions are held constant (creep).

To fully understand the theory of elasticity it is necessary to define *stress* and *strain.* The two concepts will be explained in the following:

2.3.2 Stress

Stress (σ) is defined as force (F) acting on a cross-section (surface) area (A). When applying SI units, stress is denoted in Pascal [Pa] which corresponds to Newton per square meters [N/m2]. The Greek letter sigma is used as a notation for stress:

$$\sigma = \frac{\mathrm{F}}{\mathrm{A}} = \frac{F}{\pi r^2} \tag{2.1}$$

If a sample exposed to a force differs in size of its cross-section areas, then the stress will depend on the position within the sample. This is because the force is equal in both cases, but when the area reduces, the stress in turn will increase. A further division of one cross-section into numerous of subsections may cause the force to vary from one subsection to another (see Fig. 2.2). It is then necessary to describe the stress state at a specific point P, which is referred to as local stresses. When considering a cylindrical shape (e.g. chalk cores which are applied in the experimental work of this thesis), forces can act in either axial or radial direction.

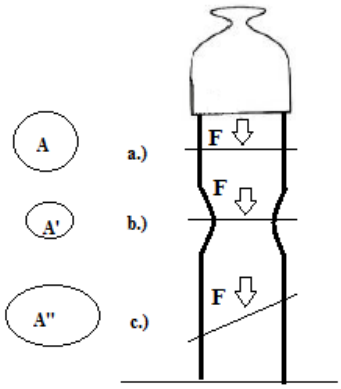

Figure 2.2: Illustration of a weight causing a force to act on a pillar. When the cross-section area is smaller (A'), the stress will be larger here than for the situation in (A).

2.3.3 Strain

Strain is when a material is deformed as a result of being exposed to external forces (stress). It is thus a measure of deformation, and strain represents the displacement between particles in an object compared to a reference length. We can distinguish between two different types of strain; elastic or plastic. *Elastic strain* is when a material recovers from deformation and return to its original shape, after the stress have been removed. *Plastic strain* on the other hand, occurs if stresses exceed a certain threshold value. This is known as the elastic limit or yield, and the deformation is now irreversible.

The dimensionless quantity of strain is called elongation, and is usually given as a percentage. It is defined as:

$$\varepsilon = \frac{L - L\prime}{L} \qquad (2.2)$$

where L is the original length of the cylinder prior to compression, and L' is the new length when it has been deformed (see Fig 2.3).

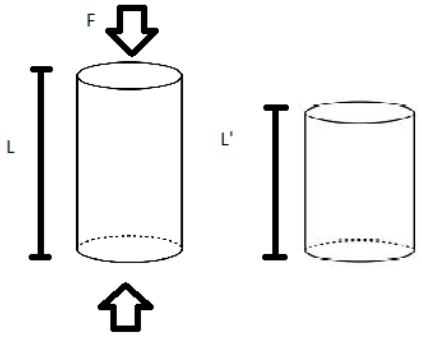

Figure 2.3: Deformation of a cylinder (e.g. chalk core) caused by an axial force F.

2.3.4 Stress -strain relations

Some materials can act in a linear elastic matter when they are exposed to certain amounts of loads. When such a material is under stress it can start to deform, but return to its original shape if the load is removed; it is said to behave elastically. However, it is only up to a specific limit that the rock structure is able to recover. The limit is often referred to as the yield point and indicates a transition from elastic to plastic phase. This means that if the material is under a substantial amount of stress and loaded beyond what it can bear, the material will no longer return to its original shape but be permanently deformed (see Fig. 2.4)

The Bulk modulus, or K-modulus, is an elastic coefficient used to determine the relationship between stress and volumetric strain during hydrostatic loading. It is a measure of the materials ability to resist compression and is defined as:

$$K = \frac{\sigma_h}{\varepsilon_v} \tag{2.3}$$

The hydrostatic stress is the same in x, y, and z-direction: $\sigma_h = \sigma_x = \sigma_y = \sigma_z$

The volumetric strain (total strain from all directions) can be defined as:

$$\varepsilon_v = \varepsilon_x + \varepsilon_y + \varepsilon_z \tag{2.4}$$

and with the assumption of isotropy during hydrostatic loading:

$$\varepsilon_v = 3\varepsilon_A \tag{2.5}$$

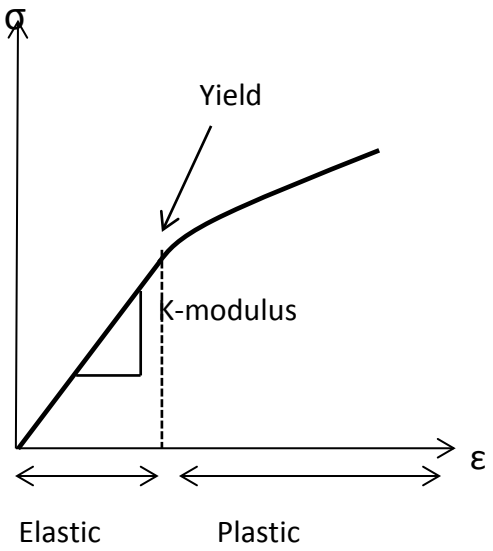

Figure 2.4: Stress-strain relationship. If the material is loaded beyond the yield point, it will be permanently deformed and is no longer able to recover to its original state.

2.3.5 Creep

Creep is defined as a time-dependent deformation that may occur when materials are subjected to constant stress. It is a molecular process, so by increasing the temperature the process becomes faster. Since the stress states are changing, creep is divided into three different phases: transient, steady state and accelerating.

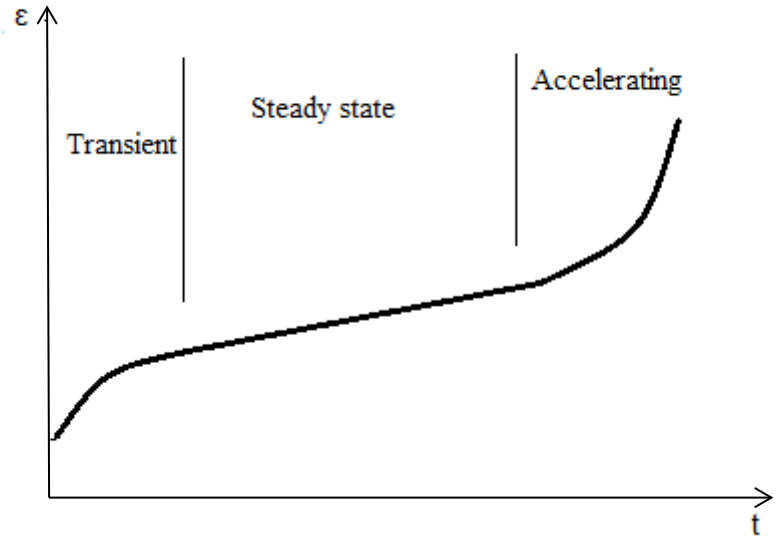

Figure 2.5: Strain versus time for a material which undergoes the three stages of creep.

The first stage is called *transient* (or primary) creep and here the rate of deformation decreases with time. If at this stage we remove the load, i.e the stress is reduced to zero, the deformation will also decrease to zero eventually. After the transient period the rate of deformation is getting more constant and evened out. This is called the *steady state* (or secondary creep). What differentiates the steady state from the primary is that if the applied stress now is reduced to zero, the deformation will still remain; the material is unable to recover and return to its original state. The last stage is called the accelerating (or tertiary) creep. As seen from figure 2.5, the deformation rate increases rather quickly with time. This final period rapidly leads to failure of the material.

2.4 Water weakening

2.4.1 Water weakening of chalk in general

When the Ekofisk field first started producing by pressure depletion, it led to formation compaction and seabed subsidence. This was beneficial for the field, as it contributed to sweep the oil out of the reservoir. After the primary-production phase ended, it was necessary to apply an enhanced oil recovery method to secure future production. Water injection started in 1987 as a countermeasure to prevent further compaction and to maintain the reservoir pressure, but even after this solution was introduced the compaction still continued. It seemed like the sea water reacted with the chalk and thus weakened the rock (Austad, Strand, Madland, Puntervold, & Korsnes, 2008).

The water weakening phenomenon has in the last previous years been devoted extensive attention. It is now well known that the mechanical strength of the rock varies, depending on the type of pore fluid being used for saturation. If the chalk is dry or saturated with oil, the yield curve will be significantly larger than if water is the saturating fluid.

2.4.2 Mechanisms affecting the chalk-fluid interaction

Various mechanisms have been suggested to explain how the rock is affected mechanically by the pore fluid. (Gutierrez et al., 2000) divide the mechanisms into three groups: capillary effects, chemical effects and physico-chemical effects.

Capillary effects occur at the interface between rock grain surfaces in contact with a pore fluid; hence a fluid surface tension is created. This happens when chalk rock is contacted by water (wetting phase) and for oil or gas (non-wetting) as water is introduced. When chalk is dried, it is not fully possible to remove all the water initially present in the small pores. As a consequence, there will be a contact pressure between the grains due to capillary meniscus created by the water bound in the pores. Since water molecules are mutually attractive (cohesive), a relatively strong force is induced. This in turn results in the grains being “pulled together” and thereby strengthens the chalk rock. However, if more water is introduced, the capillary meniscus will burst and the contact pressure and surface tension vanish, as the

water fills up the voids. Now the chalk will be considerably weaker than before. Oil on the other hand, which is a non-wetting fluid, would not have an impact on the capillary bonds. Yet, experiments performed by (Risnes & Flaageng, 1999), concluded that other mechanisms besides capillary effects must have an impact on the water weakening phenomenon. The experimental results showed that when a core was saturated with methanol, which is miscible with water, the capillary forces disappeared. However, it appeared that this core was a lot stronger than for the previous case with water saturation. This observation revealed that the chalk strength also is affected by the type of fluid present in the pores, and not solely by the capillary forces.

Physico-chemical effects occur when a fluid reacts with chalk, and triggers a chemical reaction referred to as stress-corrosion. The effect causes relatively strong chemical bonds to eventually be replaced by weaker ones, as this effect occur just at chalk crack tips. Such a severe reduction in strength will make the cracks even more exposed to stress and they tend to propagate more easily. However, both the capillary effects and physico-chemical effects did not seem to contribute enough to weaken the chalk in the extent that was being observed.

Chemical effects are another mechanism that can affect compaction, and include mineral dissolution, precipitation, substitution and intergranular pressure solution. Some minerals tend to break up and dissolve when they are exposed to liquids. This occurs to chalk which consists of calcium carbonate, $CaCO_3$, as water make the rock dissolve into Ca^{2+} and CO_3^{2-} ions. Dissolution can result in the grain sizes becoming smaller, and thereby decrease the strength of the contact pressure. Tests carried out by (Butenuth & De Freitas, 1989) showed that when calcite reacts with an aqueous fluid, not only does minerals dissolve and hence reduces the mass, but the distinctive surface properties of the crystal can also be altered. Change of the calcite surface area, is another effect that might occur when an aqueous fluid is introduced. Precipitation of minerals on the other hand can increase the rock strength, as the pores are cemented and clogged (Wan, Alsaleh, & Labuz, 2011). Lately, extensive research has been carried out to investigate the chemical effects further. This mechanism seems to be responsible for the observed deformation of chalk, although many aspects are still quite mysterious.

2.4.3 Chemical water weakening

The effect of various flooding brines on the mechanical strength of chalk has been thoroughly investigated during the last years. Studies have shown that when the injected brine contains ions like Ca^{2+}, Mg^{2+} and SO_4^{2-} in addition to chalk mineralogy itself, this can influence the rock properties and hence make it unstable. (Madland et al., 2011) flooded different types of chalk with $MgCl_2$ and observed that independent of the chalk type, the effluent had a reduced amount of magnesium ions in combination with an increased concentration of calcium. Previous experiments done by (Reidar et al.) suggested that

magnesium substituted calcium ions within the chalk core if sulfate was present. However, more recent studies done by (Madland et al., 2011) showed that cores flooded solely by $MgCl_2$ experienced a substantial amount of deformation comparable with that of sulfate. Despite that the new facts contradicted the hypothesis, it could not be completely ruled out. Further research done with $MgCl_2$ as flooding brine detected a great loss of magnesium within the core, as well as calcium production by analyzing the effluent. When the total magnesium and calcium concentration found in the effluent was added, the concentration was approximately the same as of the original injected $MgCl_2$. This observation can point towards a substitution process of one magnesium ion lost, in relation with one calcium ion being produced. Further calculations were executed to evaluate the amount of mol left within the core, and the number turned out to exceed the highest adsorption potential. It seemed like another process besides substitution contributed to this major loss of magnesium. A possible explanation could be that magnesium in the injected brine precipitated and formed new mineral phases. By analyzing the SEM (Scanning Electron Microscope) images, it appeared that magnesium-bearing minerals such as clay-like silicate and carbonate were present in the core. The precipitation of this new minerals can in turn cause an enhanced weakening of the chalk (Madland et al., 2011).

(Megawati, Hiorth, & Madland, 2012) made some further observations concerning the effect of sulfate on mechanical behavior of chalk. The experiments were performed on three different outcrops cores from Liege, Stevns Klint and Kansas. It appeared that when sulfate was adsorbed from the pore water it induced a negative surface charge, which in turn created a disjoining pressure between the grains. The effect proved to be dependent on temperature in addition to sulfate concentration, and affected both the mechanical properties and creep when the temperature was 130°C. It also revealed that even though the outcrops were different, all the chalk types experienced a reduced yield and bulk modulus under the mentioned conditions compared to that of NaCl-flooded cores. However, when the temperature was lowered to 50°C none of the cores seemed to have a remarkable difference in yield and bulk values.

3 Methodology – experimental equipment and procedure

3.1 Test material

The experimental work has the purpose to simulate the same conditions found in the North Sea chalk formations. However, the type of chalk used is not directly retrieved from the Ekofisk field. This would naturally be the most desirable situation, but reservoir chalk is rather limited and therefore not appropriate to use for test cores. Difficulties during coring and subsequent treatment before experiments can damage the core samples, so having a substitute for this reservoir chalk is more convenient. Outcrop surface chalk is available in large quantities many places in Europe, having similar properties such as permeability and porosity as certain North Sea chalk formations. In these experiments, outcrop chalk from the quarry of Obourg near Mons Belgium has been used.

Outcrop chalk	Obourg Saint Vaast
Quarry	Mons
Age	Campanian lower

Table 3.1: Properties of Mons chalk

3.2 Preparation of core samples

Several core samples were drilled out from the Mons chalk block by using a drilling machine with a cylindrical core bit, as shown in figure 3.1. The chalk block was placed inside the container and water is flushed through the core bit, while drilling.

Figure 3.1: The drilling machine used to extract the cores from the Mons chalk block.

Since the results from each experiment are compared later on, it was important to mark the top and bottom sides for every core sample. In this way it was possible to make sure that the flooding direction (vertically upwards) was equal for all tests. Before cutting and shaping could start, water had to be removed from the cores after the drilling process. The chalk cores were placed into a heating cabinet at 90°C until they became completely dry, which normally will take around 24 hours.

When using a drilling machine the cores get a relatively rough and uneven surface. This can be corrected by shaping the cores in a turning lathe (see Fig.3.2), making the surface smoother by "peeling" off the outer layer. The shaping process is done twice to remove one additional layer so the predetermined diameter also is achieved of 38,1 mm. After measuring up the desirable length, approximately around 70-80 mm, the core samples were cut using a cutting machine (see Fig.3.3). Cutoff end pieces from every core were saved for comparison after experiments.

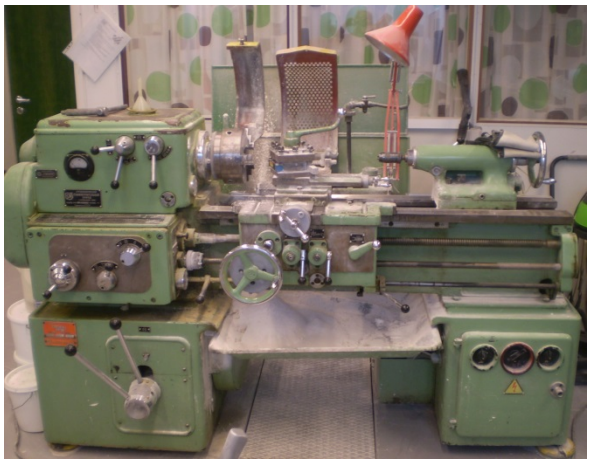

Figure 3.2: The turning lathe machine

Figure 3.3: The cutting machine (Struers Discotom-5)

In this experiment both intact and fractured core samples would be analyzed and compared. To create a fracture, the chalk core is mounted in the lathe and a hole is drilled straight through the center with a diameter of 2 mm. Dry weight of each individual core was then measured on a scale, followed by saturation of the cores with distilled water in a vacuum chamber. After being saturated, all cores had to be weighed once more to be able to estimate the porosity.

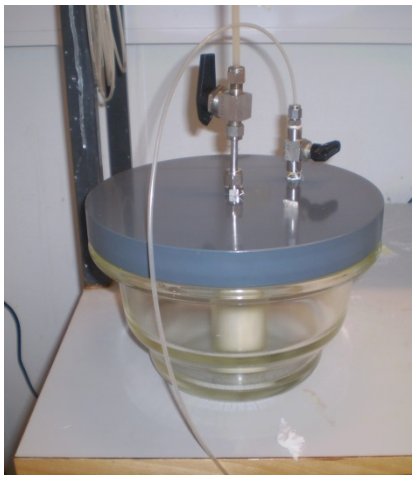

Figure 3.4: Saturation of a core sample in the vacuum chamber.

Knowing the length, diameter, dry and saturated weight of each core, the porosity could be calculated using equation 3.1 to 3.3.

Bulk volume (total volume) of the cylindrical core:

$$V_b = \frac{\pi D^2 L}{4} \tag{3.1}$$

where

D: Diameter of the core
L: Length of the core

To find the void space, i.e. the pore volume in the chalk core, the dry and saturated weight had to be applied using equation 3.2:

$$V_p = \frac{W_{sat} - W_{dry}}{\rho_f} \tag{3.2}$$

where

W_{sat} = weight of saturated core sample
W_{dry} = weight of dry core
ρ_f = density of the saturating fluid

When the bulk – and pore volume are determined, the porosity can be calculated. It is a dimensionless quantity, but it is normally given in percentage:

$$\phi = \frac{V_p}{V_b} * 100 \quad (3.3)$$

5 core samples with and without a fracture was used in this experiment. For the test cores to be comparable it was necessary that they had similar properties, such as length and porosity. The cores are listed in table 3.2:

Chalk core	Length [mm]	Diameter [mm]	Dry weight [g]	Saturated weight [g]	Bulk volume [ml]	Pore volume [ml]	Porosity [%]
OB SV 12 (fractured)	68.54	38.12	123.56	156.75	78	32.25	41.34
OB SV 9 (intact)	70.1	38.13	126.57	160.54	80	33.072	41.34
OB SV 4 (fractured)	68.81	38.13	125.23	156.96	78.35	31.73	40.49
OB SV 6 (intact)	70	38.11	127.65	160.24	79.8	32.57	40.81
OB SV 18 (fractured)	68.28	38.09	122.94	155.86	77.77	32.03	41.18

Table 3.2: Core samples used in the experiments

3.3 Brines

Different types of brines were mixed and used to flood through the core samples. By knowing the composition of the fluids, it was possible to determine if some chemicals were precipitated or dissolved in the chalk core after flooding. In these experiments the cores were first saturated with 0.657M NaCl, and flooded for six days with this same type during testing. After six days the initial brine was replaced into either SSW or 0.219M $MgCl_2$, and flooded with this until the end of the experiment (see table 3.3):

Chemical	Synthetic seawater (SSW) [g/l]	0.657 M NaCl [g/l]	0.219 M $MgCl_2$ [g/l]
NaCl	23.38	38.4	
Na_2SO_4	3.41		
$NaHCO_3$	0.17		
KCl	0.75		
$MgCl_2 . 6H_2O$	9.05		44.50
$CaCl_2 . 2H_2O$	1.91		

Table 3.3: Recipes for the brines used in the experiments.

When mixing brines, distilled water was filled into a flask of either one or two liters, to have the desirable amount. Salts were then added one at the time, while the flask was standing on a magnetic stirrer (see Fig. 3.5). When all the chemicals in the recipe were added, the solution had to be mixed for about an hour for all the salts to be properly dissolved. After mixing the brine was filtrated using a filter paper with mesh size of 0.65 µm (see Fig. 3.6). The pH was then tested for all brines using a SevenEasy METTLER TOLEDO pH meter (see Fig. 3.7).

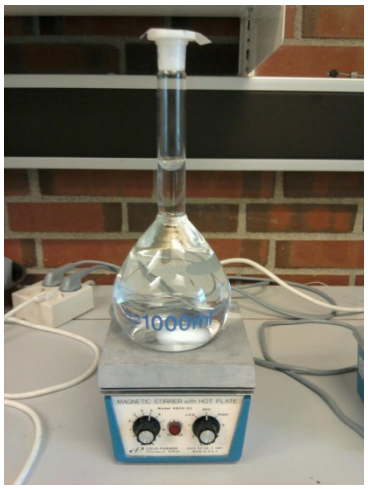

Figure 3.5: Magnetic stirrer and volumetric flask

Figure 3.6: Filtration of brine

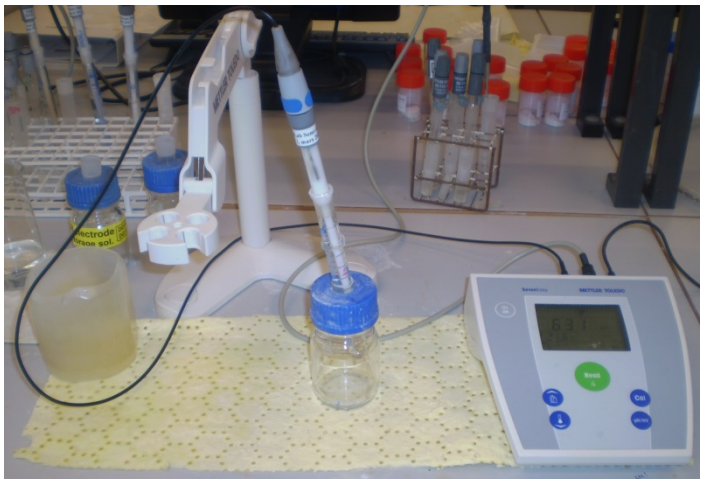

Figure 3.7: SevenEasy METTLER TOLEDO pH meter, used for measuring the pH of the different brine types.

3.4 Equipment

3.4.1 Triaxial cell

The experiments were carried out by using a high pressure, high temperature (HPHT) triaxial cell (see Fig. 3.8). This cell made out of steel makes it possible to perform tests under the same conditions found in a reservoir.

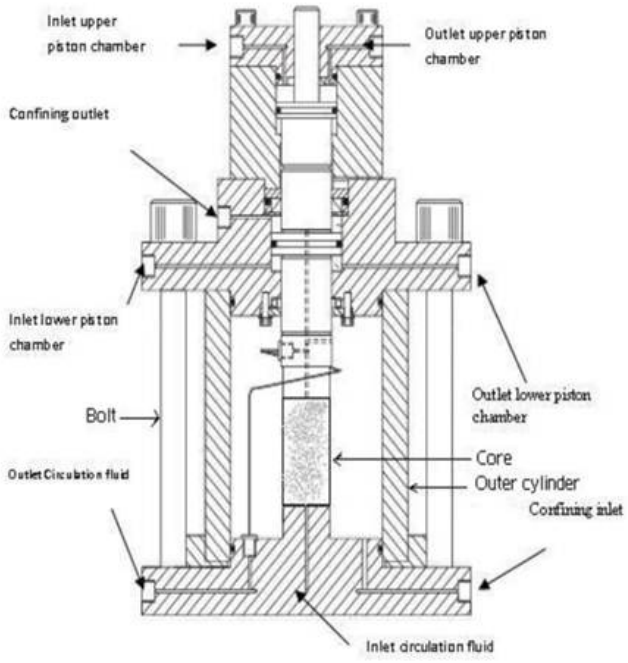

Figure 3.8: HPHT triaxial cell (Merete Madla Vadland)

3.4.2 High pressure pumps

The triaxial cell was operated by three high pressure *Gilson Pumps, Model 307 HPLC* (see Fig. 3.9). One pump called the *flooding pump,* is controlling the rate of the brine passing through the test core. To ensure that force is acting equally in all directions around the core, a second pump is necessary called the *confining pump*. For the core to be deformed in the axial direction, a piston is lowered on top of it. The force needed is supplied by a third pump called *the piston pump*.

Figure 3.9: Gilson pumps, Model 307 HPLC.

The pumps can be controlled manually, but is mainly operated by using a computer program called *LabVIEW*. Flooding rates and maximum pressure values can be set and changed as desired during testing. These values are logged in an excel sheet, together with information such as temperature, axial deformation and elapsed time. The latter is varied and adapted through different stages of the experiment. For instance it can be beneficial to log every minute in the beginning during hydrostatic loading, and increase the time interval to 3-5 minutes when reaching the creep phase. By using the Labview software program it is possible to always keep track on how the mechanical behavior of the core sample is changed when flooding with various brines. A graph constantly provides updated results over axial movement versus time, or other information needed while the experiment is running.

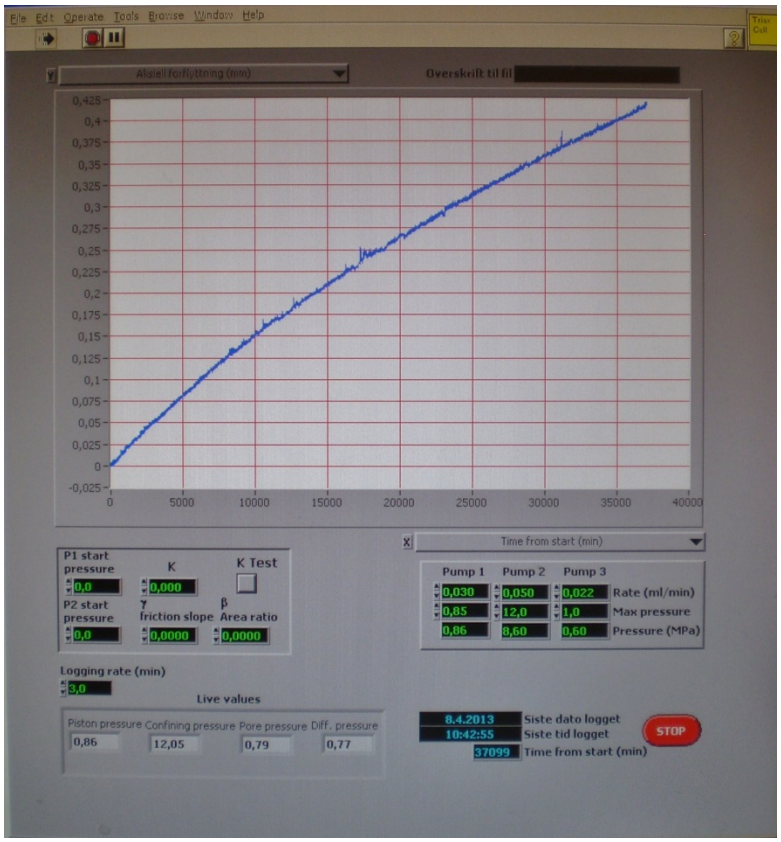

Figure 3.10: The LabVIEW program makes it easy to control and monitor flooding rates, time intervals, maximum pressures and displays the results graphically.

3.4.3 Chemical testing

While the experiments were running, it was constantly collected water samples of the brine flooded through the core. By doing this it was possible to perform a chemical analysis of the effluent water and measure the anion and cation content by using a Dionex Ion Chromatograph ICS-3000 (see Fig. 3.11). Prior to every test it was sampled a glass of original brine. In this way it was possible to compare the initial ion concentration, with the content found in the water samples collected during testing. When the core is flooded with various chemicals it can affect the chalk and contribute to a change in the ion concentration. This again can have an impact on the mechanical strength of the core sample. Before the effluent water could be analyzed it had to be diluted 500 times by using a Gilson Syringe Pump, Model 402 (see Fig. 3.11). The diluted water was next filtered and put into 1.5 ml glasses by using a syringe.

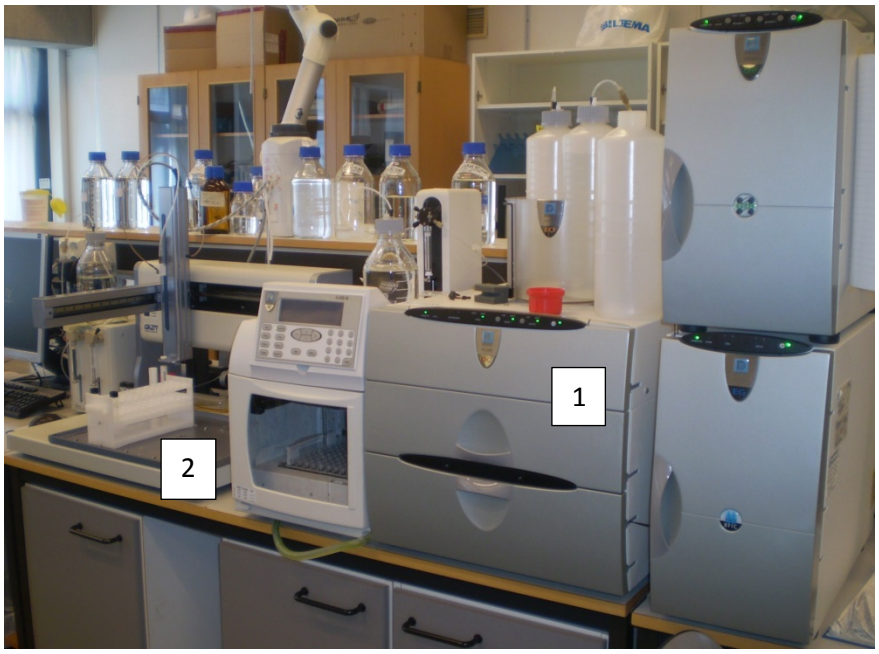

Figure 3.11: Equipment used for diluting water samples and performing chemical analysis of the anion and cation concentration. 1: Dionex Ion Chromatograph ICS-3000. 2: Gilson Syringe Pump, Model 402

3.5 Procedure

The same procedure was followed for every experiment and done over a period of three days (steps). Before the test core could be installed in the triaxial cell, it had to be put inside a cylindrical container and placed into the vacuum chamber. While the air was being sucked out, the chalk core was saturated with NaCl. For the core to be "cleaned" properly it was left in the brine overnight. All tests were submerged in this same brine type in the beginning of each experiment, and flooded with this the first six days.

Step 1

The first step was to put the saturated core in a shrinking sleeve and place it in the center (i.e. the bottom piston) of the triaxial cell (see Fig 3.12). The brine would then, later in the process, be flooded through a small hole underneath the core and vertically upwards. A heating gun was used for the sleeve to get properly tightened around the core, and thus prevent any leakages. Next, a steel cylinder was mounted around the core and created a gap between the center and the outer part of the cell. Marcol oil was filled in the annulus until it covered the core completely, and a steel lid was fitted on top.

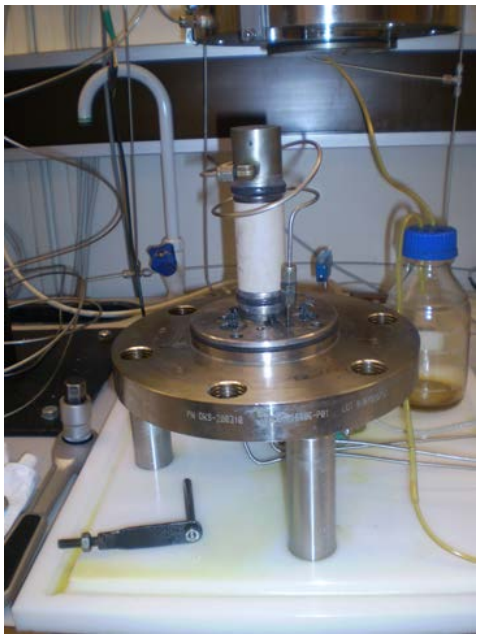

Figure 3.12: Core in a shrinking sleeve, mounted on the bottom piston in the triaxial cell.

To increase the temperature of the system, a heating jacket was placed around the steel cylinder and 6-9 bolts secured the lid with the bottom parts of the cell. The last step was to place an LVDT (linear voltage displacement transducer) on top of the cell which measures axial movement and hence the axial deformation of the core (see Fig 3.13).

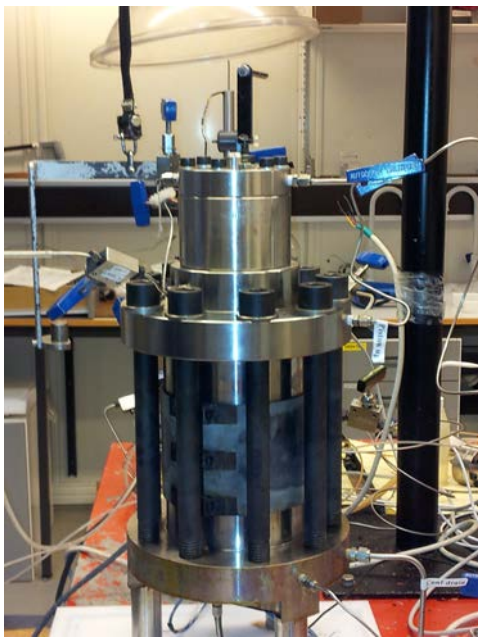

Figure 3.13: The final set-up of the triaxial cell before experimental testing. The heating jacket is mounted on the steel cylinder and 6-9 bolts connect the upper and lower parts of the cell.

LabVIEW was started on the computer to control the different pumps and what flooding rates to use. Next the confining pump was turned on and the maximum pressure was set to 0.5 MPa.

Step 2: build up confining and pore pressure

While the confining pressure had stabilized at 0.5 MPa as preset in LabVIEW the day before, the pore pressure was kept at zero. The next step was then to increase both the confining and pore pressure gradually until it reached 1.2 MPa and 0.7 MPa respectively. First, a pore pressure regulator was manually set to 0.1 MPa while the confining pressure was adjusted to 0.6 MPa. After the pressures stabilized, the same procedure continued with increasing the pressures stepwise, always keeping the confining pressure 0.5 MPa above the pore pressure. This was important to prevent any leakages from the core sample and into the oil. When the pressures eventually reached its maximum at a level of 1.2 MPa and 0.7 MPa, the flooding pump started to transport brine through the system. What flooding rate to be used for each test was determined by calculating 1 PV/24 hours, normally ranging from 0.022-0.023 ml/min.

Finally, the heating element was turned on and the temperature slowly started to increase towards 130 °C, the same temperature found at reservoir conditions. As the temperature is elevated - causing the confining fluid (oil) in the annulus to be heated up - the oil will expand and a relief valve had to be connected to the confining outlet. By adjusting the valve, some of the excess oil will be forced out from the cell and thus keep the confining pressure stable. When the final temperature is reached, the piston is lowered carefully on top of the core to prevent any damage. The core is then flooded with its specific rate in the next 24 hours.

Step 3: hydrostatic loading and creep

Finally, the last steps in the procedure are called the hydrostatic loading phase followed by the creep phase. The confining outlet is closed as the confining rate is set to 0.05 ml/min. The confining pressure is then gradually increased until the core reaches yield at a pressure of 12 MPa. After the yield phase is passed, the test is left to creep.

During the whole test phase, water samples were constantly collected of the brine used for flooding through the core sample. An original water sample of the brine was saved prior to testing to ensure a reference for comparison later on. In this way the ion composition in the water could be analyzed and any potential dissolution and precipitation determined.

3.6 Porosity measurements

After the mechanical testing was finished, the core was put in a heating chamber for drying. When the sample was completely dry, a caliper was used to measure the length of the core in three different areas to gain an average value. Next, the core was marked (see Fig. 3.14) along its respective length to make it able to distinguish the core slices after cutting them with the cutting machine (see figure 3.3) - and connected with numbers ranging from zero (inlet) to seven (outlet). The diameter was then measured three different places for every marked number along the length to find the average value for each slice.

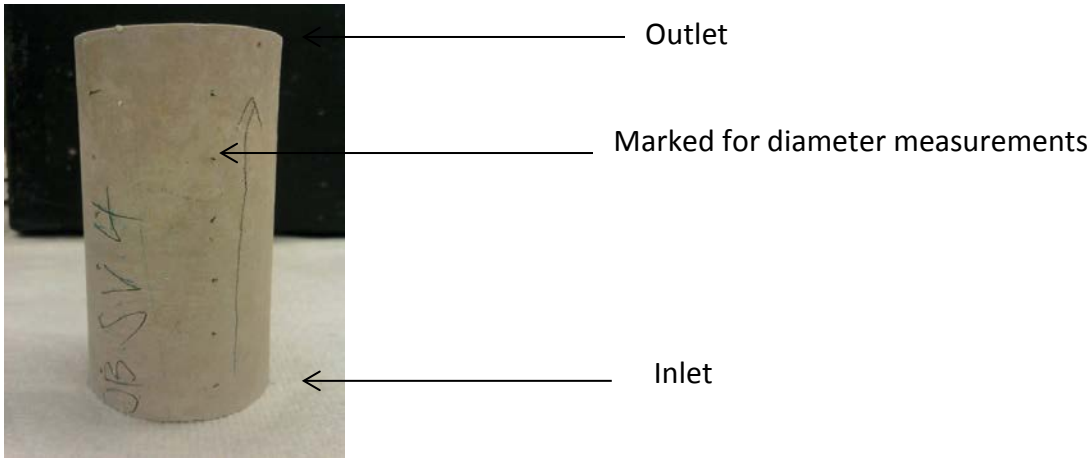

Figure 3.14: the core sample was marked all the way from inlet to outlet to find the average diameter.

Afterwards, the core slices was measured on a scale to find the weight of each slice and then put inside an AccuPyc II 1340 Gas pycnometer (see Fig. 3.15). The pycnometer calculated the samples volume and standard deviation, and made it possible to find the density of each slice after testing.

Figure 3.15: AccuPyc II 1340 Gas pycnometer.

When all the measurements were completed, the porosity of each tested core sample could be compared with obtained values prior to testing. In this way, it was possible to see if the core had changed its porosity during the experiments.

There are two different methods to calculate the porosity. The first way bases the calculations simply on the change in bulk volume prior to and after testing, and assumes that nothing has happened to the chalk grains (mechanical). The second method on the other hand, takes into consideration that possible changes has occurred to the grain structure due to chemical reactions caused by the flooding brine (chemical). To get an overview, the different methods are presented in table 3.4 and 3.5:

Initial porosity of the core sample *prior to testing*:

Mechanical	Chemical + mechanical
$\phi = \frac{V_p}{V_b}$	$\phi_0 = 1 - \frac{M_s}{\rho * V_b}$

Table 3.4: mechanical and chemical formulas to calculate the initial porosity of the core

where

V_p: pore volume [cc]
V_b: bulk volume prior to testing [cc]
M_s: mass of core sample prior to testing [g]
ρ: density of core sample prior to testing [g/cc]

Porosity *after testing*:

Mechanical	Chemical + mechanical
$\frac{\phi_0 - \varepsilon_V}{1 - \varepsilon_V}$	$\phi_{after} = 1 - \frac{M_{s(A)}}{\rho_{pycno} * V_b'}$

Table 3.5: mechanical and chemical formulas to calculate the porosity of the core after testing

where

ε_V: change in volumetric strain [cc]
$M_{s(A)}$: mass of core sample after testing [g]
ρ_{pycno}: density of core forund from pycnometer [g/cc]
V_b': bulk volume after testing [cc]

A more detailed description of the procedure is presented in the following:

The new bulk volume of the core after testing is calculated by using the formula of truncated cone volume:

$$\frac{1}{3} * \pi(r_1^2 + r_1 * r_2 + r_2^2)h \quad (3.4)$$

where

r_1: radius of core slice by the inlet
r_2: radius of the second core slice moving towards outlet
h: height of individual slice

Then the volume of all slices was summed together to find the total bulk volume, V_b', after testing.

Next, the change in volumetric strain prior to and after testing could be calculated:

$$\varepsilon_V = \frac{V_b - V_b'}{V_b} \quad (3.5)$$

where

V_b: bulk volume prior to testing
V_b': bulk volume after testing

Then the density ρ prior to testing was found:

$$\rho = \frac{M_s}{V_b - V_p} \quad (3.6)$$

where:

V_p: pore volume
M_s: solid mass of core prior to testing

Finally, *the initial mechanical porosity* was calculated by:

$$\phi = \frac{V_p}{V_b} \quad (3.7)$$

And *chemical and mechanical porosity* combined:

$$\phi_0 = 1 - \frac{M_s}{\rho * V_b} \quad (3.8)$$

This value was compared to the *porosity values for the core after testing*:

mechanical:

$$\phi_{after} = \frac{\phi_0 - \varepsilon_V}{1 - \varepsilon_V} \tag{3.9}$$

Chemical and mechanical porosity combined:

$$1 - \frac{M_{s(A)}}{\rho_{pycno} - V_b'} \tag{3.10}$$

where

$M_{s(A)}$: mass of core after testing
ρ_{pycno}: density measurements based on the pycnometer

The density found from the pycnometer was calculated by weighted average of each slice:

$$\rho_{pycno} = \frac{\rho_1 * V_1}{V_{tot}} + \frac{\rho_2 * V_2}{V_{tot}} + \ldots \tag{3.11}$$

where

ρ_1: density of individual slice based on pycnometer volume and measured weight
V_1: volume of each slice found by pycnometer
V_{tot}:total volume of all slices measured in pycnometer

4 Results

The experimental work in this thesis was performed in collaboration with another master student, (Abubeker, 2013). A total number of five chalk cores were prepared and tested in the same manner. However, three of the cores had a hole of 2 mm in diameter drilled all the way through the center while the remaining two were intact. The purpose for this thesis was to observe how the mechanical strength of the chalk is affected when a core is fractured as opposed to being intact, when flooded with different types of brines. In addition, it was of interest to detect precipitated minerals within the core by analyzing SEM (scanning electron microsopy) and effluent water.

First, the cores went through two different mechanical tests; hydrostatic and creep, keeping a constant temperature of 130°C. After the mechanical tests were ended effluent water was collected continuously while flooding and a chemical test were later performed to analyze the effluent. Finally, the densities of the cores were measured to find if there had been any porosity alteration compared prior to testing. The brines used in the experiments were 0.657 M NaCl, synthetic seawater (SSW) and 0.219 M $MgCl_2$.

All core samples were drilled out from the same Mons chalk block and named after the chalk type; “Obourg Saint Vaast”, shortened “OB SV”. The cores OB SV 12, OB SV 4 and OB SV 18 had the induced fracture, whereas OB SV 9 and OB SV 6 both were intact.

For clarity it should be mentioned that OB SV 18 (fractured) were flooded with 0.657 M NaCl throughout the whole mechanical testing period, while the other cores were flooded only the first six days with this particular brine and thereby had their brine substituted. The reason was to use the OB SV 18 core as a reference when comparing the experimental results after testing, and observe how the cores were affected by the various types of brines. OB SV 12 (fractured) and OB SV 9 (intact) had the brine changed to SSW and OB SV 6 (intact) and OB SV 4 (fractured) were changed to 0.219 M $MgCl_2$.

As mentioned earlier, the experimental work in this thesis was performed in cooperation with (Abubeker, 2013). Two tests at the time were run in parallel with one core having a fracture whereas the other was intact – flooded with either 0.219M $MgCl_2$ or SSW.

4.1 Fractured cores

4.1.1 Mechanical test

All the cores were flooded with a rate equal to 1 Pore Volume (PV) per day, and data were logged throughout the whole hydrostatic phase and creep phase. The core data for the fractured chalk cores are presented in table 4.1:

Chalk core	Length [mm]	Diameter [mm]	Dry weight [g]	Saturated weight [g]	Bulk volume [ml]	Pore volume [ml]	Porosity [%]
OB SV 12	68.54	38.12	123.56	156.75	78	32.25	41.34
OB SV 4	68.81	38.13	125.23	156.96	78.35	31.73	40.49
OB SV 18	68.28	38.09	122.94	155.86	77.77	32.03	41.18

Table 4.1: Core data of the fractured core samples

4.1.1.1 Hydrostatic loading

All the core samples were flooded with 0.657M NaCl during hydrostatic loading, and the axial stress and strain were measured. Yield point is found during the hydrostatic phase, as the stress-strain curve starts to deviate from the linear trend. The procedure to find the numerical value for the yield point is demonstrated for OB SV 18 in figure 4.1. Two linear trend lines are drawn through the elastic and plastic phase of the stress-strain curve and extrapolated into a cross section. From the cross section, the yield point can now be found by the dotted red line intersecting the “axial stress” axis. Yield values for all the cores are listed in table 4.2. The bulk modulus, or K-modulus, was found from the slope of the stress-strain curves in the linear elastic area and by applying equation 2.3. The bulk modulus measures a materials ability to resist uniform compression with the assumption of the strain being isotropic. Porosity values, yield strength and bulk modulus varies for the different cores even though they all originate from the same quarry. Both OB SV 12 and OB SV 18 have yield strength of approximately 9.4 MPa, also having quite similar porosity values. However, OB SV 12 seem to deform more rapidly having a axial strain of 0.57% when reaching yield point – whereas OB SV 18 only has 0.47 % axial strain in the same particular point. This can also be reflected in the bulk modulus of the two cores, where OB SV 12 has a lower value. At the end of the hydrostatic test, the total axial strain is higher for OB SV 12 with a value of 1.07%, compared to OB SV 18 with a total axial strain of 0.84%. OB SV 4 on the other hand, show higher yield strength compared to the other cores, having a value of approximately 9.6 MPa. This can be because the porosity is somewhat lower, hence resulting in the core being mechanically stronger. OB SV 4 has an axial strain of 0.48 % when reaching the yield point, ending in a total axial strain of 0.81% after the hydrostatic loading. The core has relatively similar bulk modulus to the one of OB SV 18, and this can be seen from figure 4.1 as the two stress-strain curves tend to overlap.

Chalk core	Porosity	Yield strength	Bulk modulus	Total axial strain after hydrostatic phase
OB SV 12	41.34 %	9.4 MPa	0.625 GPa	1.07 %
OB SV 4	40.49 %	9.6 MPa	0.750 GPa	0.81 %
OB SV 18	41.18 %	9.4 MPa	0.753 GPa	0.84 %

Table 4.2: mechanical results from the hydrostatic phase

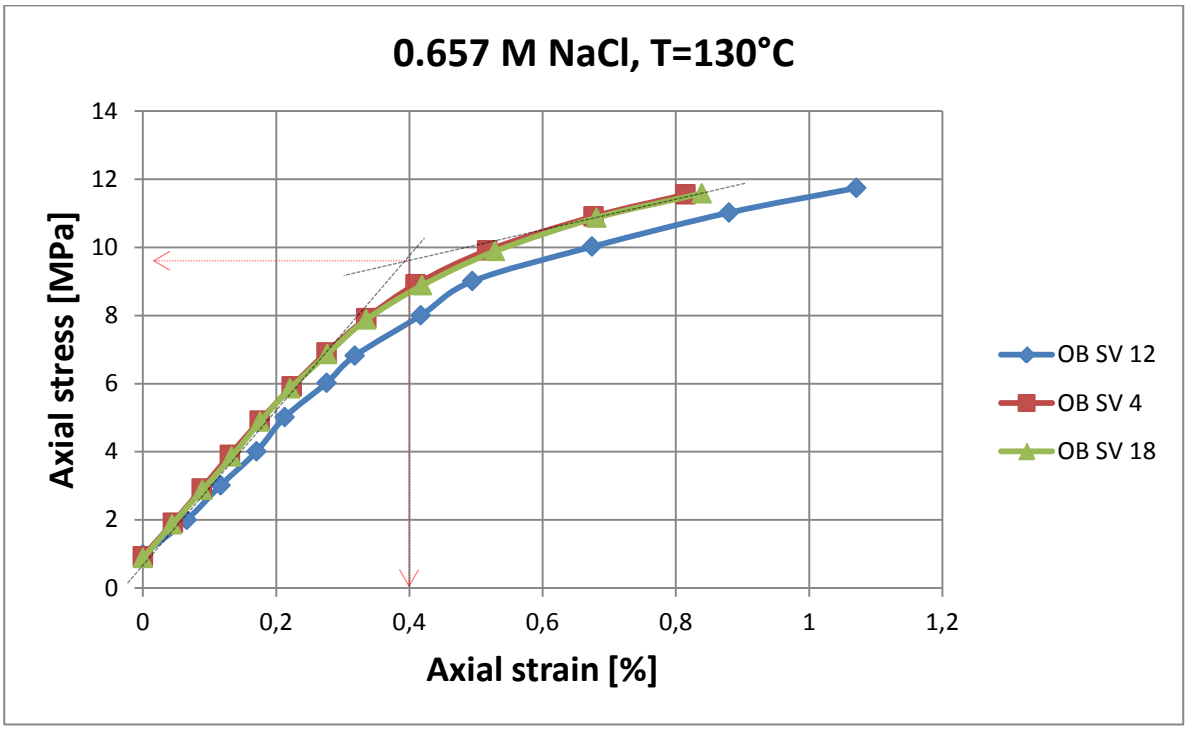

Figure 4.1: Axial stress [MPa] plotted as a function of axial strain [%], for the three *fractured* core samples; OB SV 12, OB SV 4 and OB SV 18.

4.1.1.2 Creep phase

After the hydrostatic phase, the cores were left to creep at a constant stress of 12 MPa. All the cores were flooded with 0.657M NaCl the first six days, and thereafter changed to synthetic seawater (SSW) for OB SV 12, and 0.219 M magnesium chloride ($MgCl_2$) for OB SV 4. The rate used for flooding was really low with only 0.023 PV/day passing through the core. When the creep phase was completed, DW was used in the purpose of cleaning prior to any SEM investigations and to observe if it had any influence on the strain rate. As mentioned earlier, OB SV 18 was only flooded with NaCl throughout the whole test period to have a reference of how the chalk and hence the creep is affected by the different types of brines.

To observe how the cores are deforming over time, the axial creep strain is plotted as a function of creep time. The fractured cores are first presented separately in a graph to better observe the effect of the particular brine. Later, all of the cores are presented in one graph for comparison. Time 0 represents the start of the creep phase.

Creep phase for OB SV 12 (fractured chalk) flooded with SSW

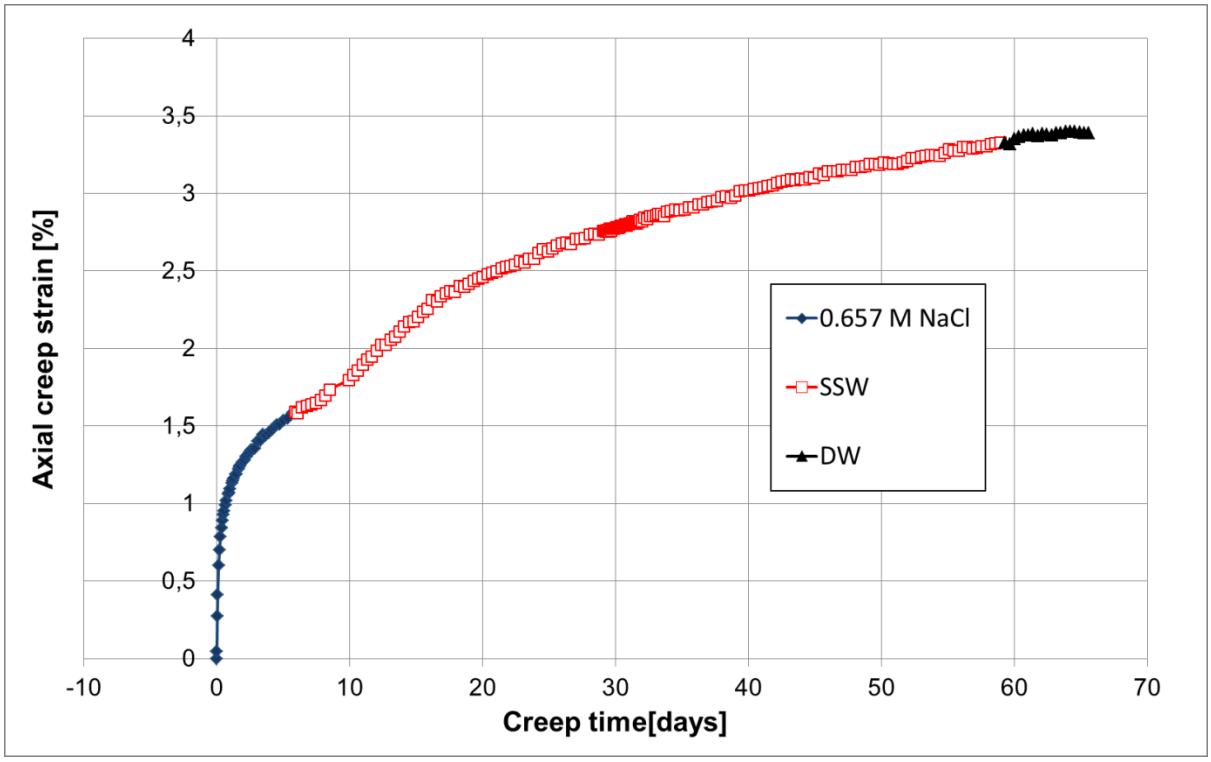

Figure 4.2: Axial creep strain [%] plotted as a function of creep time [days] for the *fractured* core OB SV 12.

OB SV 12 was flooded with 0.657M NaCl the first six days, and from the graph it can be observed that the creep reduces quite rapidly. After six days when SSW is introduced, the core has reached an axial creep strain of approximately 1.59%. The following period show a rather distinct transition as the strain rate reduces slightly in the very beginning and eventually starts to increase, resulting in a total creep strain of 3.38% after the 65 days of creep period. The core was flooded with DW during the final phase of the creep period - lasting for around 7 days – and from figure 4.2 it can be observed that the DW does not have an influence on the strain rate. The properties of OB SV 12 are listed in table 4.3:

Chalk core	**Total creep period [days]**	**Flooding fluid first 6 days**	**Brine change**	**Flooding rate [PV/day]**	**Axial creep strain at brine change [%]** NaCl-SSW	**Total axial creep strain [%]** Incl. DW
OB SV 12	65	0.657 M NaCl	SSW	0.023	1.59	3.38

Table 4.3: The particular brines used for flooding and the resulting axial creep strains.

Creep phase for OB SV 4 (fractured chalk) flooded with 0.219M $MgCl_2$

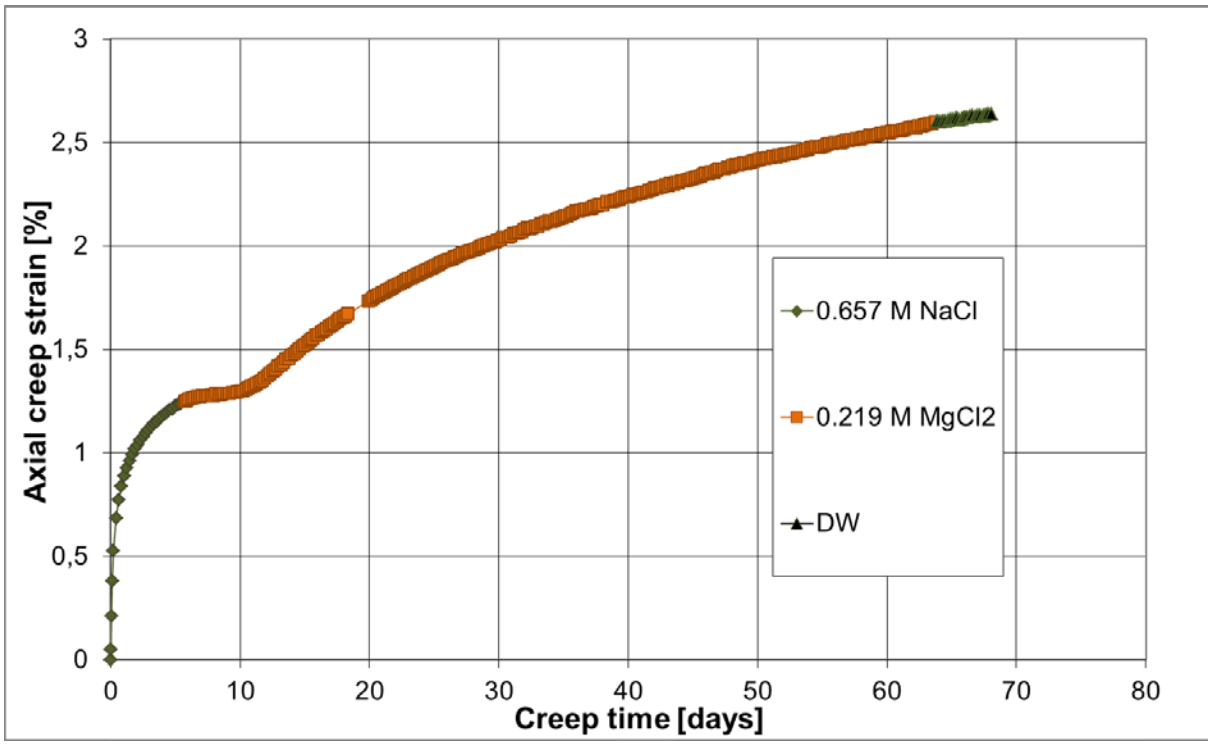

Figure 4.3: Axial creep strain [%] plotted as a function of creep time [days] for the *fractured* core OB SV 4.

OB SV 4 was flooded with 0.657M NaCl the first six days and from the graph it can be observed that the core experiences a reduction in strain rate (transient creep), from the very beginning. Just prior to the brine is substituted to 0.219 M $MgCl_2$, the axial strain has reached a level of 1.25%. After $MgCl_2$ is introduced, the creep curve show a retarding trend before it gradually increases after approximately 10 days. When the creep period has ended after 68 days of flooding, the total axial creep strain has reached 2.63%. The properties of OB SV 4 are listed in table 4.4:

Chalk core	**Total creep period**	**Flooding fluid first 6 days**	**Brine change**	**Flooding rate [PV/day]**	**Axial creep strain at brine change [%]** $NaCl$-$MgCl_2$	**Total axial creep strain [%]** Incl. DW
OB SV 4	68	0.657 M NaCl	0.219 M $MgCl_2$	0.022	1.25	2.63

Table 4.4: The particular brines used for flooding and the resulting axial creep strains.

Creep phase for OB SV 18 (fractured chalk) flooded with 0.657M NaCl: reference core

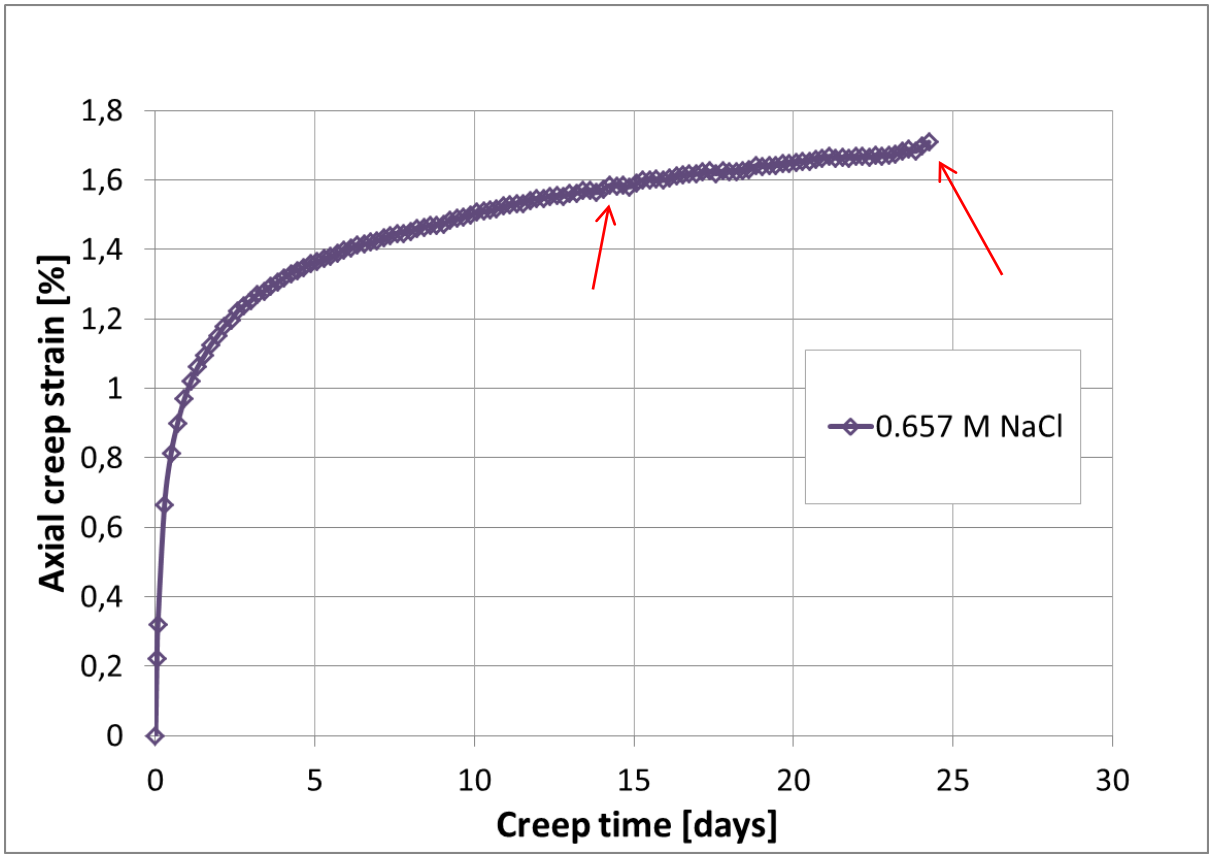

Figure 4.4: Axial creep strain [%] plotted as a function of creep time [days] for the *fractured* core OB SV 18.

OB SV 18 was flooded with 0.657M NaCl during the whole creep period. In this way it was possible to use the core as a reference, and compare the development of the axial creep strain with the cores flooded with different brines. From the graph it can be seen that the axial creep curve reduces very quickly and seems to continue into a transient and steady-state phase. However, the curve never starts to accelerate (accelerating phase) but continues in the same trend. When the creep period has ended after 24 days of flooding, the total axial creep strain has reached a level of 1.70%. The red arrows in the graph are to point out sudden "jumps" in the axial creep strain. At the far end of the curve it can look like the curve is starting to accelerate, but similar increases in creep strain are detected in earlier stages of the creep phase as well. The properties of OB SV 18 are listed in table 4.5:

Chalk core	Total creep period	Flooding fluid whole period	Flooding rate [PV/day]	Total axial creep strain [%]
OB SV 18	24	0.657 M NaCl	0.023	1.70

Table 4.5: The particular brine used for flooding and the resulting axial creep strain.

Comparison of the fractured core samples

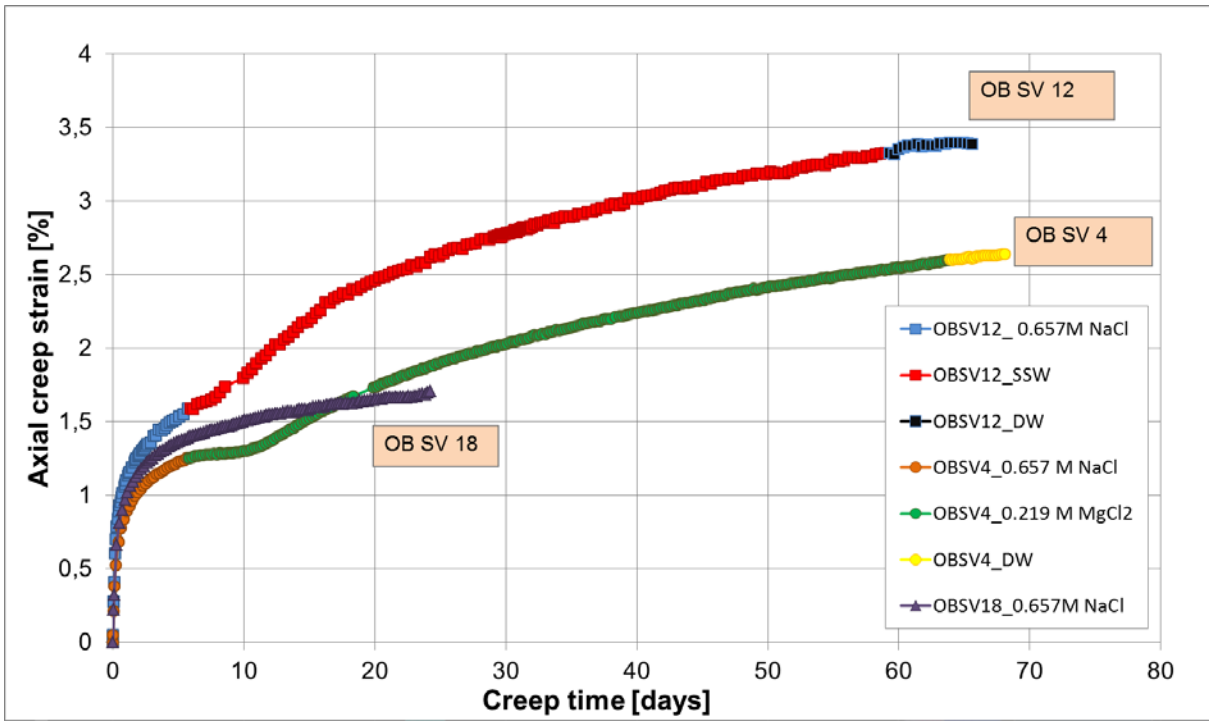

Figure 4.5: Axial creep strain [%] plotted as a function of creep time [days] for the *fractured* core samples OB SV 12, OB SV 4 and OB SV 18.

All the three core samples were flooded with 0.657M NaCl from the start of the creep phase, but OB SV 12 and OB SV 4 changed the brines after six days to synthetic seawater (SSW) and magnesium chloride 0.219M $MgCl_2$, respectively. Only OB SV 18 was flooded continuously with 0.657M NaCl throughout the whole testing period. From the graph it can be seen that all the three cores experiences a reduction in strain rate (transient creep phase) the first days when flooding with 0.657M NaCl brine. By looking closer at OB SV 18 it can be seen that the deformation of the core continues, but the curve seems to decelerate somewhat (primary creep), ending at a total axial strain of 1.70%. OB SV 12 has reached an axial creep strain of 1.59% just prior to brine change, and the creep strain increases as SSW is introduced as flooding brine. After the end of the creep period, the total axial strain for OB SV 12 ends at a value of 3.38%. OB SV 4 on the other hand, has the lowest value of axial creep strain after six days, and reaches 1.25% prior to brine change. This core switches brine to 0.219M $MgCl_2$, and the axial creep strain seems to flatten or stabilize the next couple of days before it starts to accelerate. The core ends at a total axial creep strain of 2.63%. By comparing all of the cores, they all experience a similar transient trend the first couple of days. However, OB SV 12 has a higher axial strain prior to brine change compared to OB SV 4. An explanation for this can be that OB SV 12 also experienced the highest total axial strain during the hydrostatic phase (see table 4.2). After the brine is substituted, the creep curves starts to deviate from each other and the core exposed to SSW (OB SV 12) experiences the

highest deformation compared to the other cores, but the one flooded with 0.219M $MgCl_2$ (OB SV 4) show a similar development in the creep curve (see table 4.6):

Chalk core	Total creep period	Flooding fluid first 6 days	Brine change	Flooding rate [PV/day]	Axial creep strain at brine change [%]	Total axial creep strain [%] Incl. DW
OB SV 4	68	0.657 M NaCl	0.219 M $MgCl_2$	0.022	1.25	2.63
OB SV 12	65	0.657 M NaCl	SSW	0.023	1.59	3.38
OB SV 18	24	0.657 M NaCl	---	0.023	---	1.70

Table 4.6: The particular brines used for flooding and the resulting creep strain for all *fractured* cores

4.1.2 Chemical analysis

The ion concentration was plotted as a function of time to analyze potential losses or increased amounts of the ions in the effluent brine (see Fig. 4.6-4.7).

Chemical analysis for OB SV 4

From the effluent water collected from OB SV 4, it was observed that both the chloride and sodium concentration fluctuates around their original concentration of 0.657M NaCl prior to brine change. Almost immediately after the flooding brine is switched to 0.219M $MgCl_2$, the sodium concentration drops to approximately 0,220M and gradually moves towards zero the following days. This is an expected outcome since there is no sodium in the injected $MgCl_2$ brine. The chloride also experiences a drop in concentration after the brine is changed and starts to stabilize around a value of 0.438M, which is the actual concentration of $MgCl_2$ in the flooding brine (see figure 4.6).

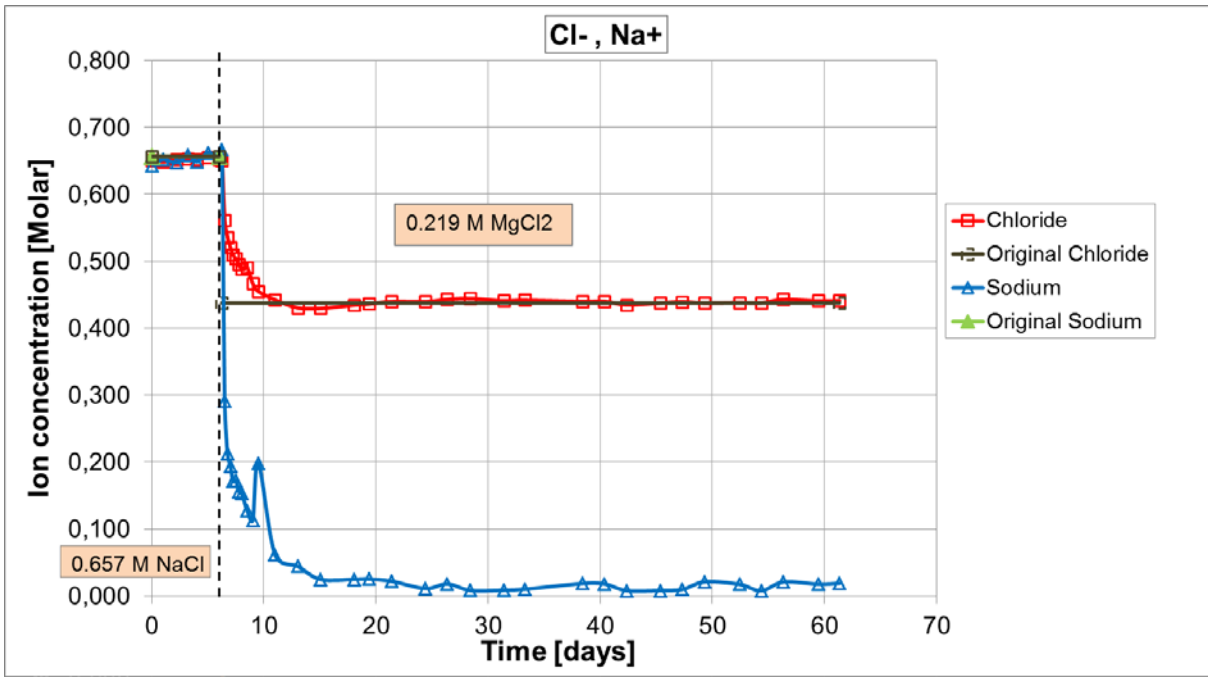

Figure 4.6: Ion concentration [Molar] for chloride and sodium, plotted as a function of time [days] for OB SV 4 (fractured).

When flooding with 0.657M NaCl there is very small amounts, if any, of calcium in the effluent brine. However, after the brine is changed to 0.219M $MgCl_2$ the calcium concentration eventually starts to accelerate, hence being produced from the chalk core. The calcium concentration tends to stabilize after 10 days at a value of 0.015M. Immediately after brine change it can be seen that magnesium is detected in the effluent as a result of the core containing a hole, and thereby causes the brine to flood straight through. The concentration then tends to gradually increase for the next 12 days. For the following period, the magnesium concentration stabilizes, but it never reaches the original magnesium concentration of 0.219M. This can be an indication that some of the magnesium is left within the core. By adding the loss of magnesium and thereby the production of calcium in the effluent, it can be seen that the total value is fluctuating around the original magnesium concentration (See figure 4.7)

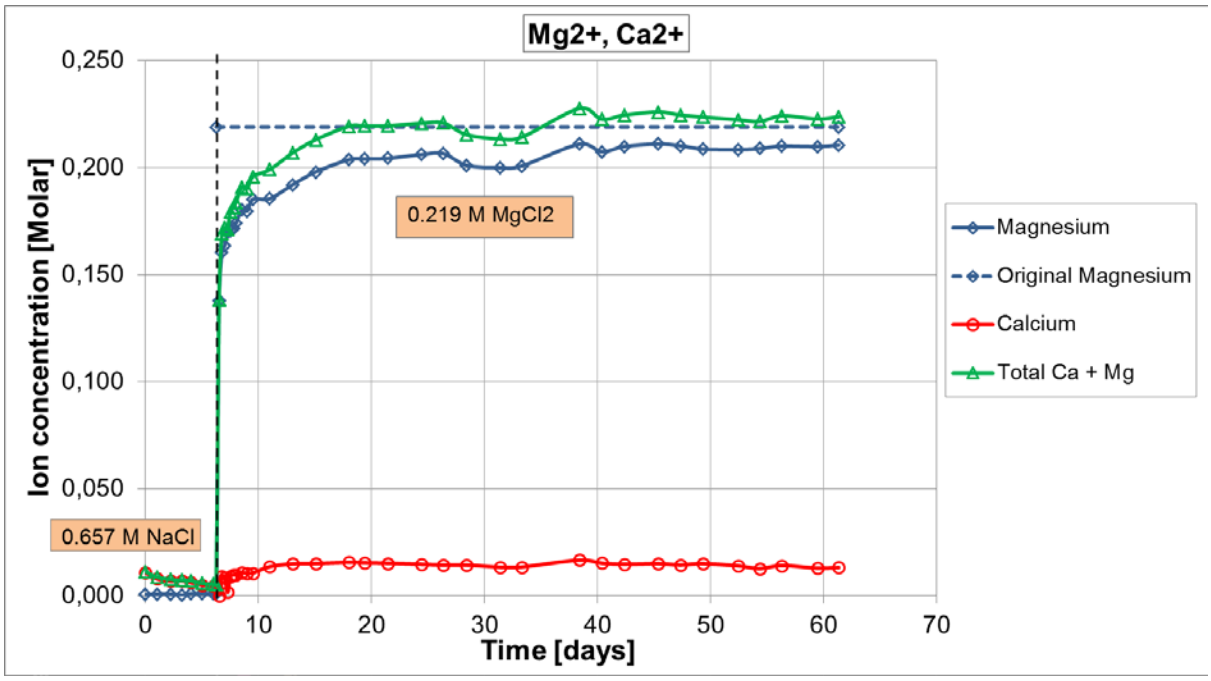

Figure 4.7: Ion concentration [Molar] for magnesium and calcium, plotted as a function of time [days] for OB SV 4 (fractured).

Chemical analysis for OB SV 12

From the chemical analysis of OB SV 12, it can be observed that immediately after the brine is changed to synthetic seawater (SSW), there is magnesium present in the effluent. The ion concentration gradually increases before it stabilizes at a level of 0.041M, but it never reaches the original concentration of 0.0445M found in the injected brine. It looks like some of the magnesium is retained within the chalk core. By studying calcium, it can be seen that there is a small amount of approximately 0.005M found in the effluent prior to brine change. When SSW is introduced, the calcium concentration starts to increase rapidly and fluctuates above its original concentration of 0.013M. The value tends to stabilize after 36 days around 0.015M, hence there is a small amount of calcium being produced. Sulfate can also be detected in the effluent right after brine change, followed by a period of fluctuation. However, after 30 days the concentration eventually reaches its original value of 0.024M. For potassium, the concentration quickly settles at its original value of 0.010M; there is no production or loss occurring. It should be noted that the large fluctuations (peaks) probably is due to a mistake with the dilution of the effluent (see figure 4.8).

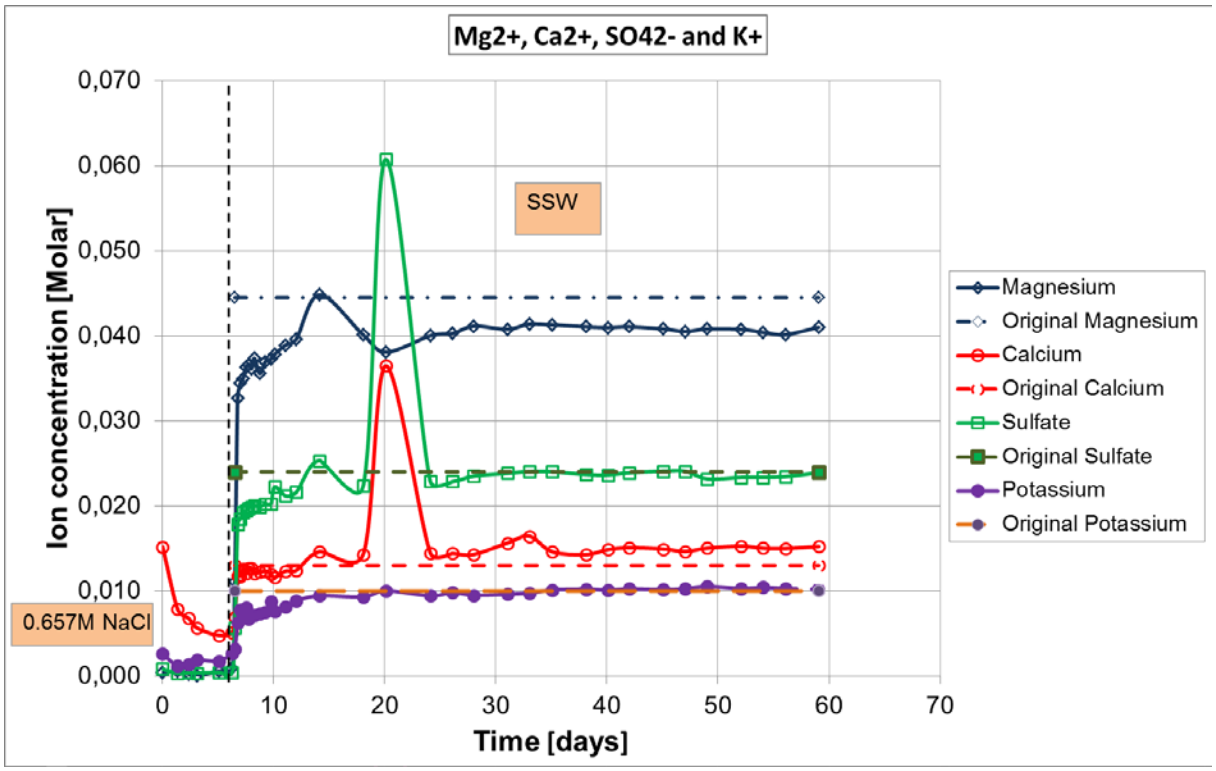

Figure 4.8: Ion concentration [Molar] for magnesium, calcium, sulfate and potassium plotted as a function of time [days] for OB SV 12.

Prior to the substitution of brine, the sodium and the chloride concentration fluctuate around their original value of 0.657M. As SSW is introduced, there is a drop in concentration for both ions, but after approximately 20 days the concentrations reaches its originals at 0.450M for sodium and 0.525 for chloride, respectively. It should be noted that the large fluctuations (peaks) probably is due to a mistake with the dilution of the effluent (see Fig 4.9).

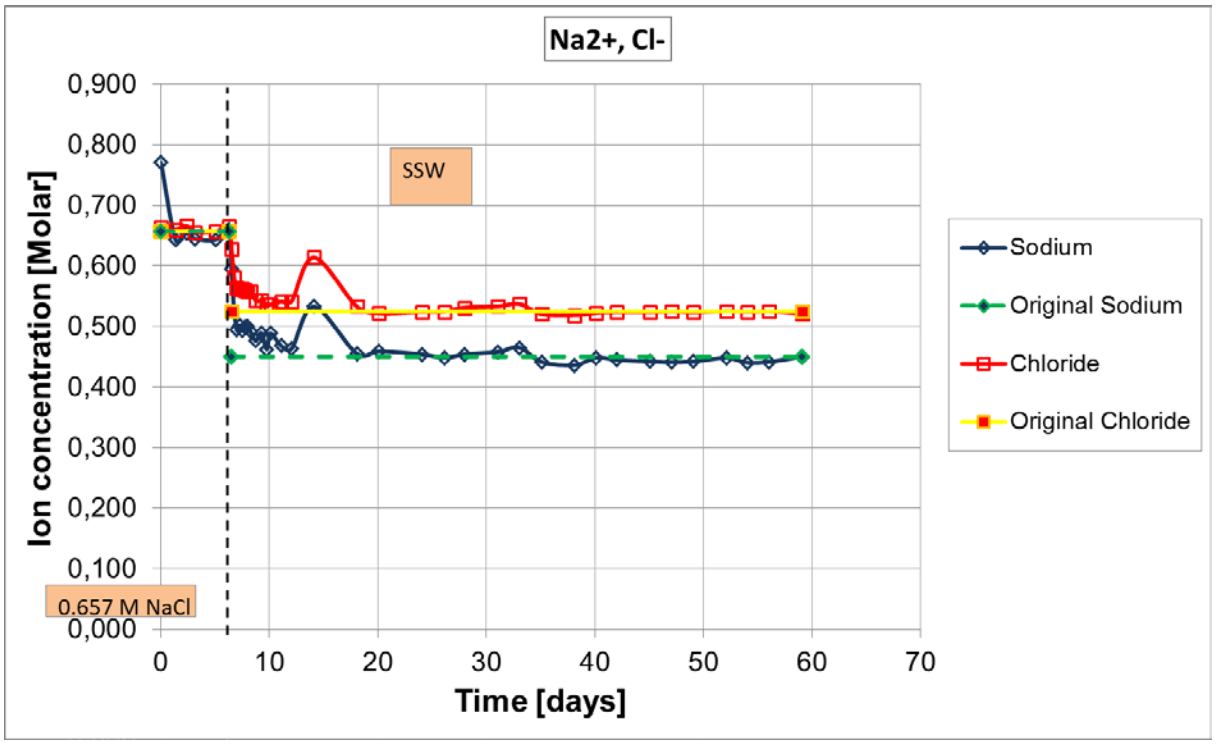

Figure 4.9: Ion concentration [Molar] for sodium and chloride, plotted as a function of time [days] for OB SV 12 (fractured).

4.1.3 Porosity measurements

The porosity measurements were based on values obtained prior to and after testing (see calculations in section 3.6). The mechanical method to measure the porosity only considers a potential change in the bulk volume of the core, whereas the chemical method includes chemical alterations of the grains inflicted by the chalk-water interactions.

By studying table 4.7 it can be observed that OB SV 4 flooded with 0.219M $MgCl_2$ experienced an increased density after testing from 2.69 [g/cc] to 2.73 [g/cc], and an additional reduction of porosity. The same thing was observed for OB SV 12 flooded with SSW as the density was increased from 2.7 [g/cc] to 2.74 [g/cc] and hence a reduction in porosity (see table 4.7).

Core Sample	V_B [CC]		ε_v	M_s [g]		ρ[g/cc]		ϕ [%]			
	B	A		B	A	B	A	B		A	
								M	M+C	M	M+C
OB SV 4 ($MgCl_2$)	78.38	73	0.0688	125.23	123.96	2.69	2.73	40.49	40.49	38.08	37.95
OB SV 12 (SSW)	78	71.5	0.0832	123.56	123.18	2.7	2.74	41.34	41.34	36.02	37.15

Table 4.7: Density and porosity values for OB SV 4 and OB SV 12, before and after experiment.

4.2 Intact cores

4.2.1 Mechanical test

All the cores were flooded with a rate equal to 1 Pore Volume per day, and measurements were taken throughout the whole hydrostatic phase and creep phase. The mechanical properties for the fractured chalk cores are presented in table 4.8:

Chalk core	Length [mm]	Diameter [mm]	Dry weight [g]	Saturated weight [g]	Bulk volume [ml]	Pore volume [ml]	Porosity [%]
OB SV 9	70.1	38.13	126.57	160.54	80	33.072	41.34
OB SV 6	70	38.11	127.65	160.24	79.8	32.57	40.81

Table 4.8: Core data of the intact core samples

4.2.1.1 Hydrostatic loading

Both the core samples were flooded with 0.657 M NaCl during hydrostatic loading, and the axial stress and strain were measured. The yield strength and bulk modulus was found as described previously in chapter 4.1.1.1. OB SV 9 experiences yield around 9.1 MPa with an associated axial strain value of 0.47% at this point, whereas the total axial strain at the end of hydrostatic phase is 0.90%. OB SV 6 starts to yield a bit later than the previous core, having a yield strength value of 9.9 MPa and axial strain of 0.53%. The total axial strain for OB SV 6 ends up at 0.81% after the hydrostatic phase (see Fig 4.10). When comparing the two cores it can be seen that OB SV 9 has a slightly higher porosity of 41.34% compared to

OB SV 6 with 40.81%. The latter shows somewhat higher mechanical strength, having a yield value of 9.9 MPa and hence a lower total axial strain of 0.81%. Yet, the bulk modulus for both core samples is approximately in the same range of about 0.6 GPa. All values are listed in table 4.9:

Chalk core	Porosity	Yield strength	Bulk modulus	Total axial strain after hydrostatic phase
OB SV 9	41.34 %	9.1 MPa	0.696 GPa	0.90%
OB SV 6	40.81%	9.9 MPa	0.685 GPa	0.81%

Table 4.9: Obtained values during hydrostatic loading for OB SV 9 and OB SV 6

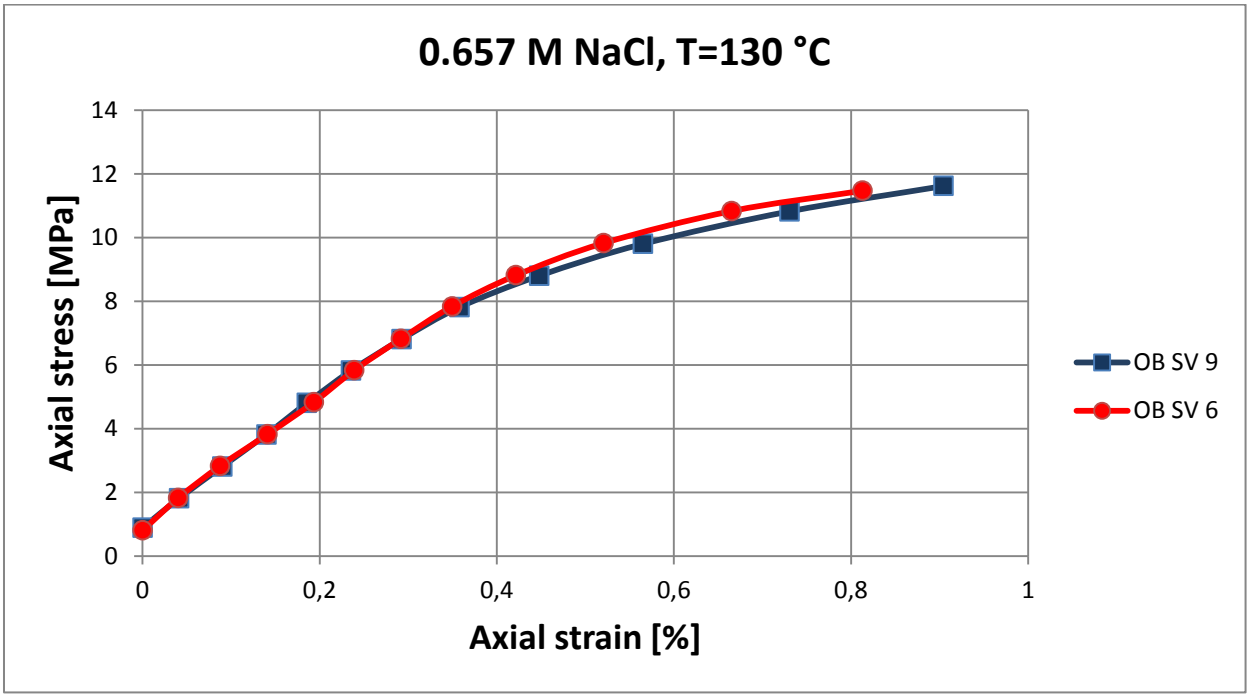

Figure 4.10: Axial stress [MPa] plotted as a function of axial strain [%] for OB SV 6 and OB SV 9.

4.2.1.2 Creep phase

After the hydrostatic phase, the cores were left to creep at a constant stress of 12 MPa. All the cores were flooded with 0.657 M NaCl the first six days, and later changed to synthetic seawater (SSW) for OB SV 9, and 0.219 M magnesium chloride ($MgCl_2$) for OB SV 6.

To observe how the cores are deforming over time, the axial creep strain is plotted as a function of creep time. The fractured cores are first presented separately in a graph to better observe the effect of the particular brine. Later, all of the cores are presented in one graph for comparison. Time 0 represents the start of the creep phase.

Creep phase for OB SV 9 (intact chalk) flooded with SSW

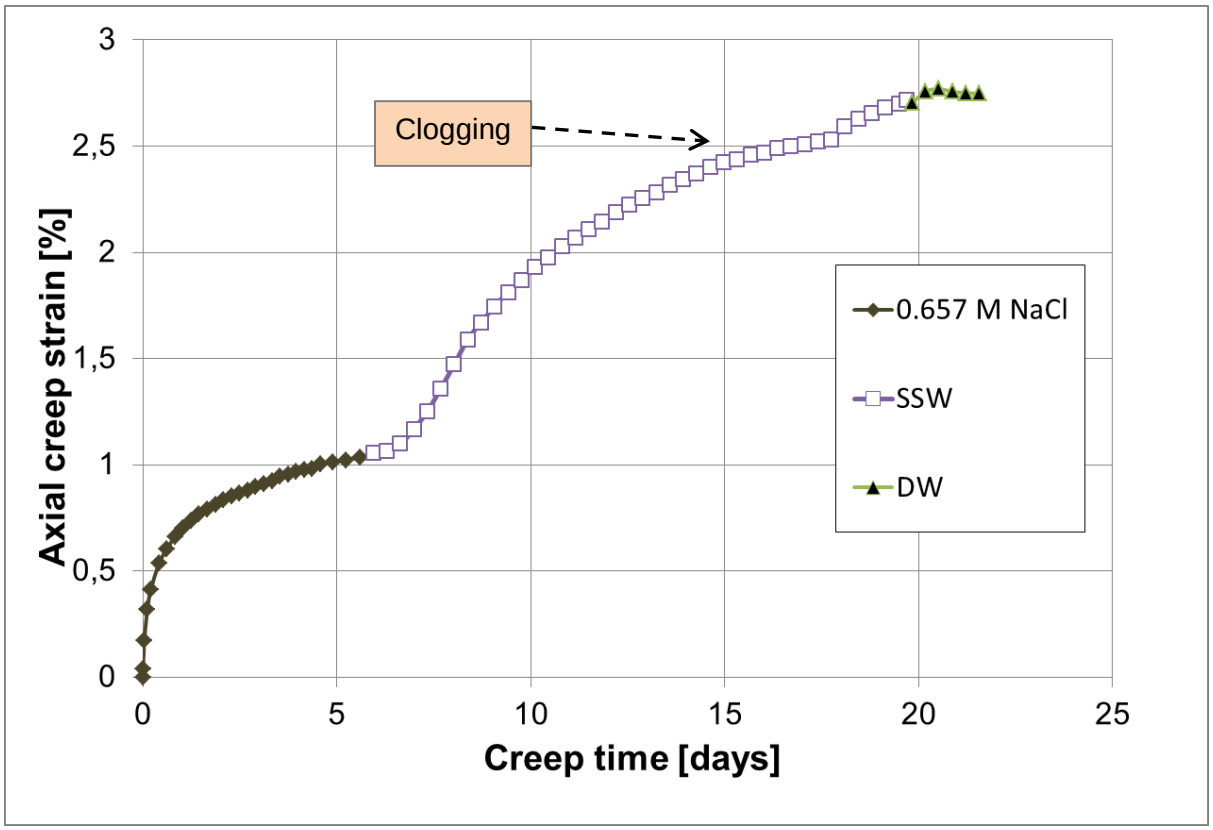

Figure 4.11: Axial creep strain [%] plotted as a function of creep time [days] for OB SV 9.

OB SV 9 was flooded with 0.657 M NaCl the first six days, and the creep curve slowly reduces into a transient creep phase (see Fig. 4.11). The axial creep strain in this particular area before the brine is substituted to SSW, is approximately around 1.05%. The following period when flooding with SSW, the creep curve shows a significantly steeper trend until it eventually experience a sudden jump. By analyzing this closer, the core sample seems to be clogged after approximately 14 days as the differential pressure, ΔP, starts to increase sharply thus causing the effective stresses to decrease. Next, the bypass was opened, the ΔP dropped and the effective stresses increased again. This can clearly be seen on figure 4.11 after 18 days of creep. When ending the creep phase after 21 days, the total axial creep strain has reached a value of 2.74%. Distilled water (DW) was flooded for around two days showing a similar axial strain trend as for the previous phase. The properties of OB SV 9 are listed in table 4.10:

Chalk core	Total creep period [days]	Flooding fluid first 6 days	Brine change	Flooding rate [PV/day]	Axial creep strain at brine change [%] NaCl-SSW	Total axial creep strain [%] Incl. DW
OB SV 9	21	0.657 M NaCl	SSW	0.023	1.05	2.74

Table 4.10: The particular brines used for flooding and the resulting axial creep strains.

Creep phase for OB SV 6 (intact chalk) flooded with 0.219M $MgCl_2$

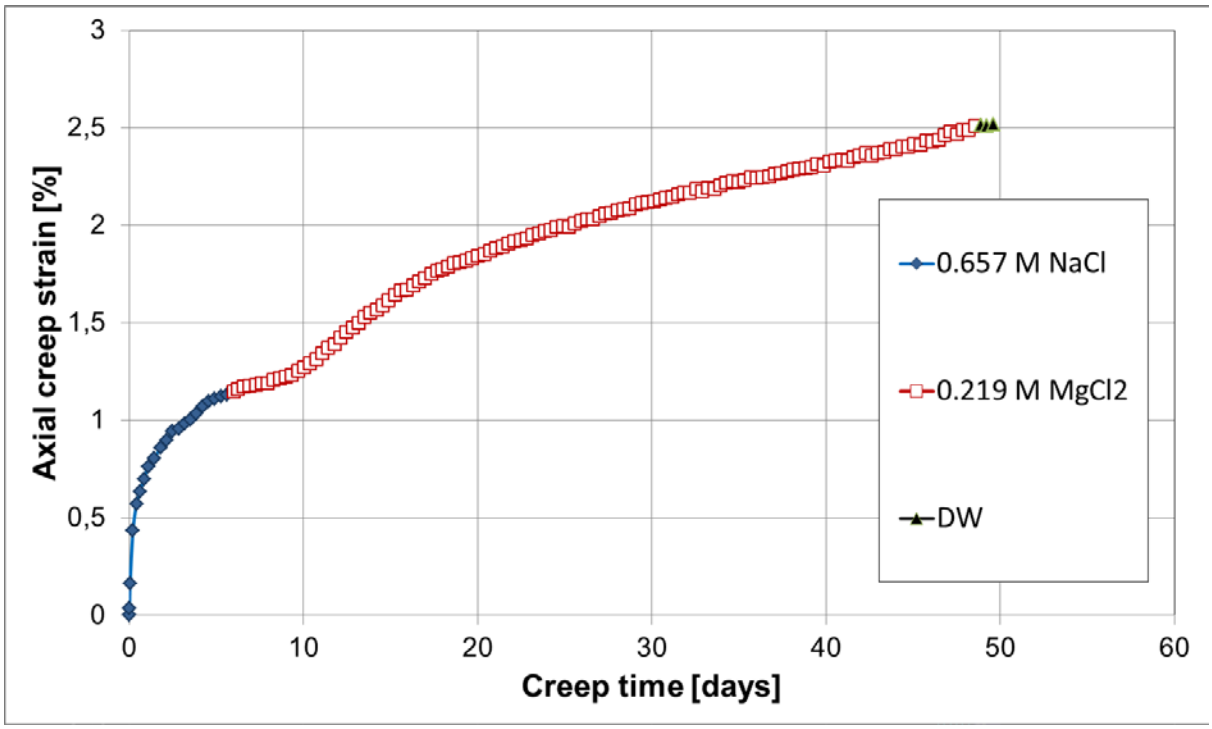

Figure 4.12: Axial creep strain [%] plotted as a function of creep time [days] for OB SV 6.

OB SV 6 was flooded with 0.657 M NaCl the first six days, and the axial creep strain starts to slow down right from the beginning of the creep phase. After the sixth day, the axial strain has reached a level of 1.15% and thereafter as shifting to 0.219M $MgCl_2$ the strain curve seems to follow a similar trend as in the previous flooding with 0.657M NaCl. However, after 3-4 days of $MgCl_2$ injection the strain rate suddenly starts to accelerate. The curve has now a much steeper trend which last approximately for 8 days. After 18 days of creep the slope gradually bends over and OB SV 6 experiences a total axial creep strain of 2.51% after 49 days of flooding. The properties of the core sample are listed in table 4.11:

Chalk core	**Total creep period [days]**	**Flooding fluid first 6 days**	**Brine change**	**Flooding rate [PV/day]**	**Axial creep strain at brine change [%]** $NaCl$-$MgCl_2$	**Total axial creep strain [%]** Incl. DW
OB SV 6	49	0.657 M NaCl	0.219 M $MgCl_2$	0.023	1.15	2.51

Table 4.11: The particular brines used for flooding and the resulting axial creep strains.

Comparison of the intact core samples

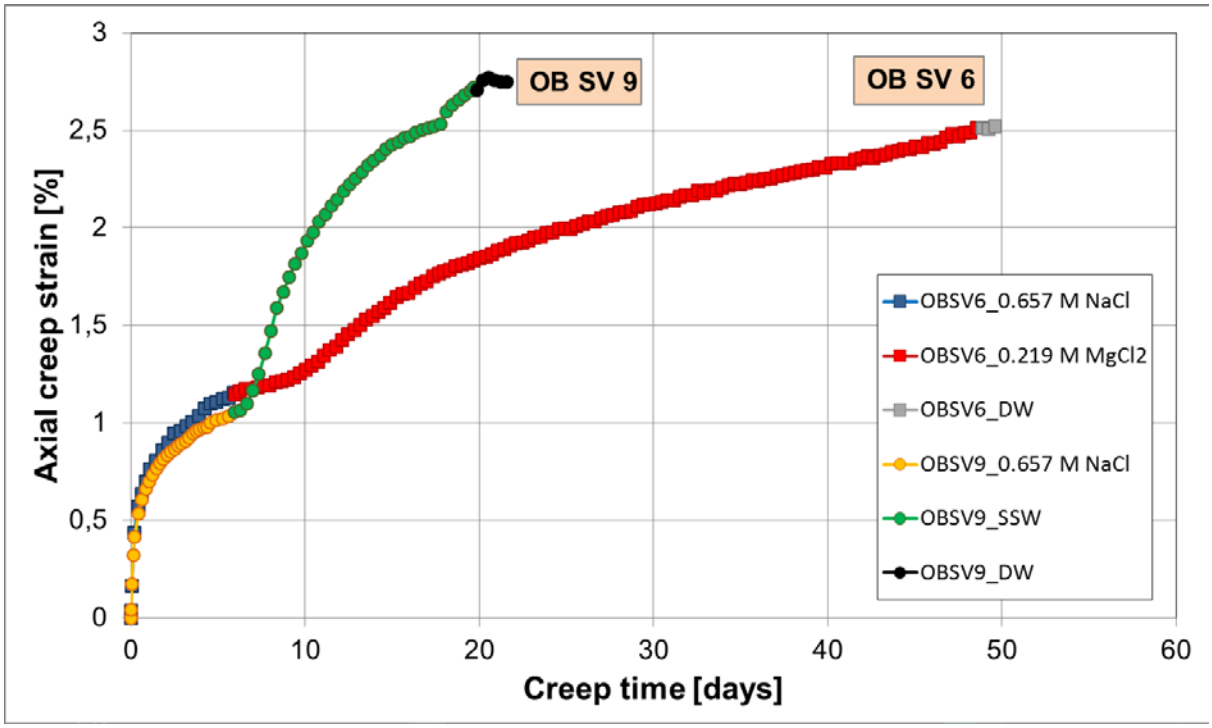

Figure 4.13: Comparison of the axial creep strain [%] as a function of creep time [days] for the fractured cores OB SV 9 flooded with SSW and OB SV 6 flooded with 0.219M $MgCl_2$.

Both of the intact core samples were flooded with 0.657 M NaCl the first six days of the creep period, but OB SV 9 seems to have a somewhat smaller response on the axial creep strain compared to OB SV 6. The latter has reached an axial creep strain of 1.15% prior to brine change, whereas OB SV 9 has a value of 1.05% in the same area. The two cores were flooded with different types of brine the following period. OB SV 9 had the brine changed to synthetic sea water (SSW), while OB SV 6 was changed into 0.219 M $MgCl_2$. It can clearly be seen from the graph that OB SV 9 flooded with SSW is affected quite strongly and experiences a total axial strain of 2.74% in a relatively short amount of creep time (days). OB SV 6 on the other hand, is also influenced when the brine is changed to 0.219 M $MgCl_2$, but the deformation in form of axial creep strain seems to develop at a slower pace. OB SV 6 has a creep period of 49 days, and the total axial creep strain reaches 2.51% (see table 4.12).

Chalk core	Total creep period [days]	Flooding fluid first 6 days	Brine change	Flooding rate [PV/day]	Axial creep strain at brine change [%]	Total axial creep strain [%] Incl. DW
OB SV 6	49	0.657 M NaCl	0.219 M $MgCl_2$	0.023	1.15	2.51
OB SV 9	21	0.657 M NaCl	SSW	0.023	1.05	2.74

Table 4.12: The particular brines used for flooding and the resulting axial creep strains.

4.2.2 Chemical analysis

The ion concentration was plotted as a function of time to analyze potential losses or increased amounts of the ions in the effluent brine. See figure 4.14-4.15:

Chemical analysis for OB SV 9

From the effluent water collected from OB SV 9, it was observed that there is a small amount of calcium present when flooding with 0.657M NaCl. When the brine is changed to SSW, the calcium concentration tends to stay in the same particular range of approximately 0.003M for the next two days. However, after eight days the concentration gradually starts to increase until it reaches a plateau around 0.026M and suddenly drops towards the original calcium concentration of 0.013M. Since the concentration of calcium in the effluent is higher than of the original concentration, there can be an indication of calcium being produced from the core. By looking at the potassium and sulfate concentration they both show a similar tendency as the one of calcium. Also here, the concentrations do not start to increase until two days after the brine is changed (day eight). For potassium, the concentration seems to be slightly above its original. The sulfate concentration on the other hand, is at its highest around 0.022M before it starts to drop gradually - but it never reaches the original concentration in the injected brine; there seems to be a loss of sulfate in the chalk core. The same development happens for magnesium, as the concentration is at zero the first two days after brine change and suddenly starts to accelerate rapidly. Like sulfate, magnesium never reaches the original concentration of 0.0445 found in the injected brine. This can also be an indication of magnesium loss within the chalk core. By adding the concentration of magnesium and calcium in the effluent, the sum starts to get close to the original concentration of magnesium after approximately 12 days (see figure 4.14).

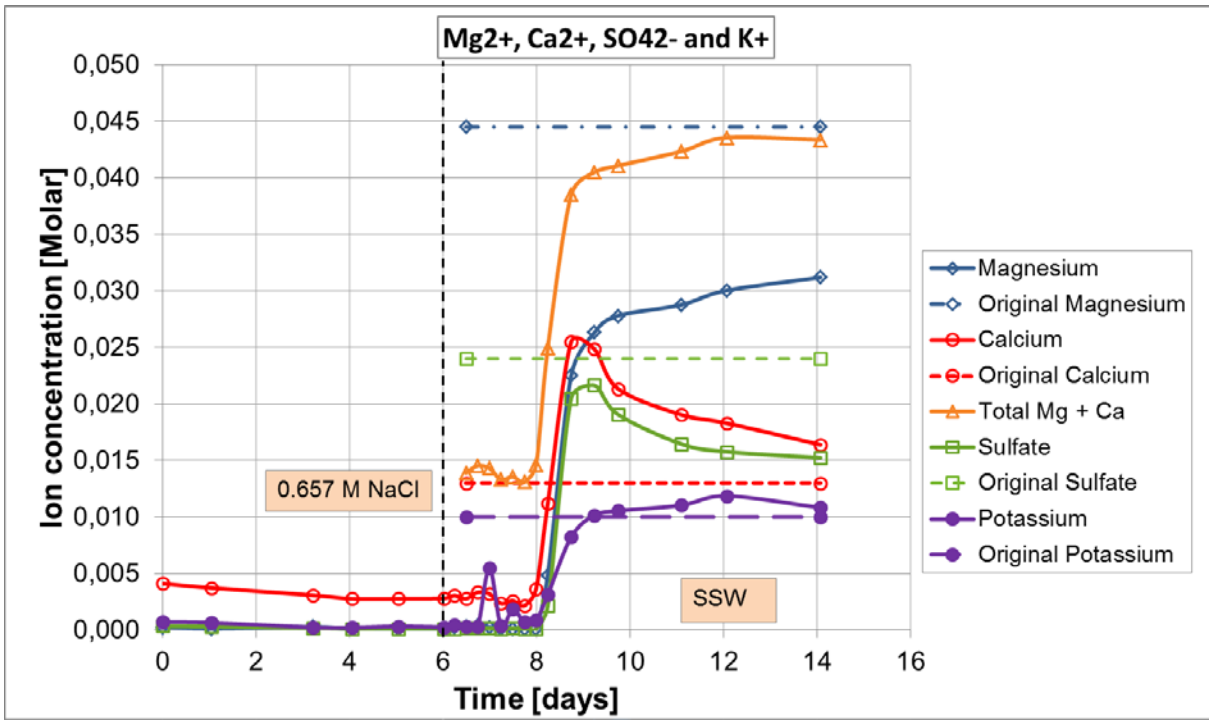

Figure 4.14: Ion concentration present in the effluent brine plotted as a function of time for OB SV 9. Magnesium, calcium, sulfate and potassium ions and their original concentrations in the SSW.

Before substitution of 0.657M NaCl, both the sodium and chloride concentration is close to their original value of 0.657M. After the brine is changed to SSW, it takes approximately one day (day seven) before the chloride concentration drops to 0.460M and gradually increases towards the original concentration the following days. Yet, it seems to be a retention of a small amount of chloride in the core as it never quite reaches the original value of 0.525M. The sodium concentration also starts to drop after day seven, but unlike chloride the sodium eventually reaches its original value of 0.450M during the course of time. This means that the concentration is the same in the effluent as for the injected brine (see fig 4.15).

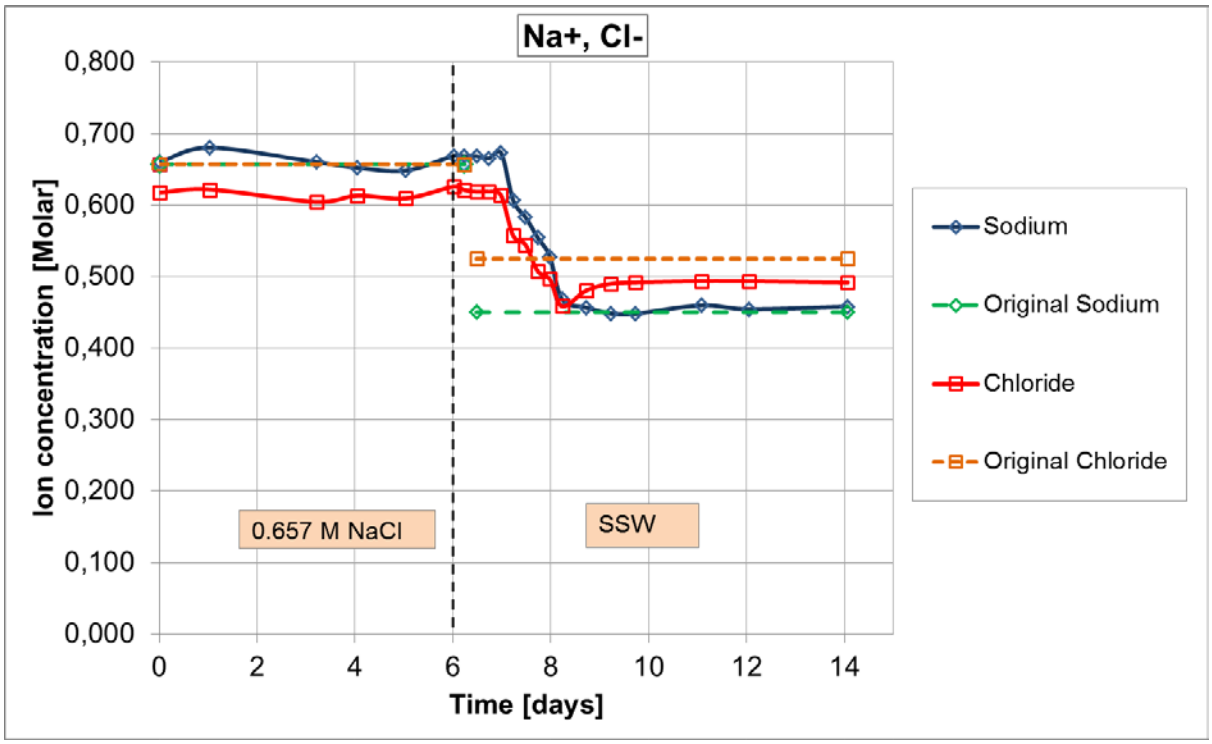

Figure 4.15: Ion concentration present in the effluent brine plotted as a function of time for OB SV 9. Sodium and chloride ions and their original concentrations in the SSW.

Chemical analysis for OB SV 6

For OB SV 6 the concentration of both sodium and chloride fluctuates around their original value of 0.657M before brine change. When the brine is switched to 0.219M $MgCl_2$, sodium concentration almost immediately starts to drop towards zero. The reason for this is because there is no sodium present in the injected 0.219M $MgCl_2$ brine. Chloride concentration follows the same trend seen for sodium right after brine change, as it continuously drops in a rapid pace. After approximately eight days (two days after brine change), the chloride concentration suddenly starts to fluctuate around a value of 0.438M - which is the same amount present in the original $MgCl_2$ (see Fig 4.16).

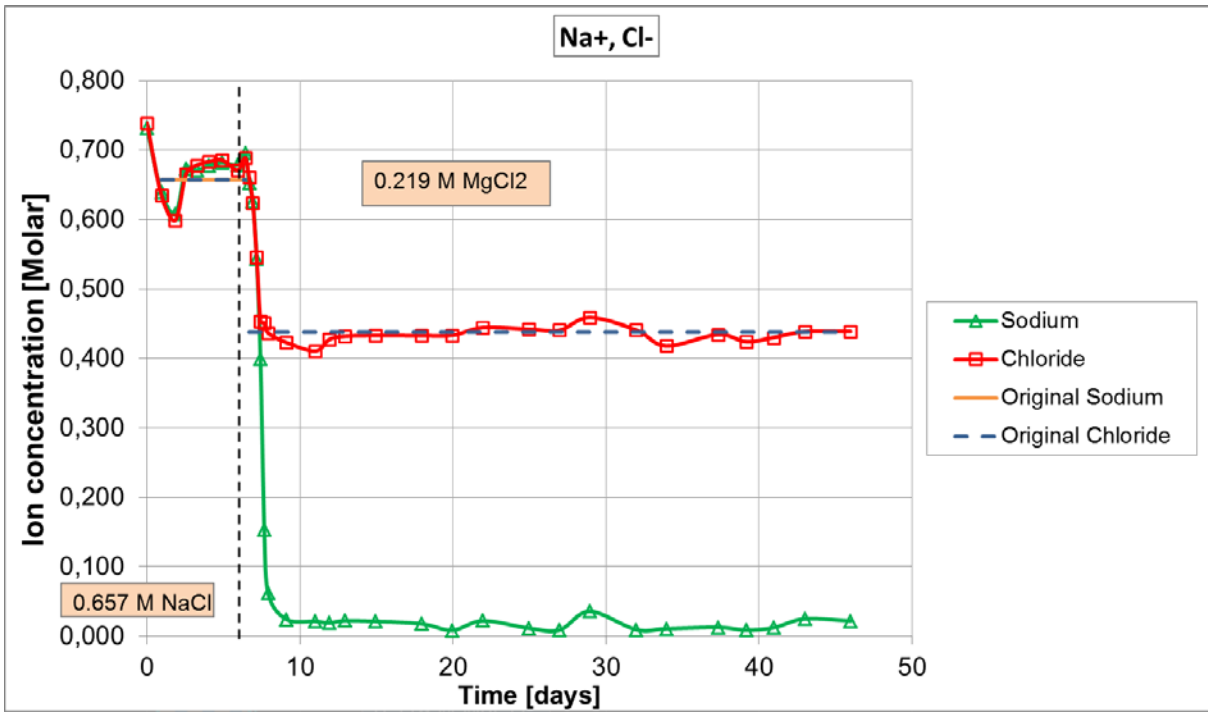

Figure 4.16: Ion concentration present in the effluent brine plotted as a function of time for OB SV 6. Sodium and chloride ions and their original concentrations.

Before the brine is substituted, there is no calcium being produced from the core sample. When the brine is changed to 0.219M $MgCl_2$ after six days, it takes approximately one day of flooding (day seven) before there is noted any calcium in the effluent. The calcium concentration is at its greatest around 0.065M before it gradually declines the following days. After a period of thirty days, the calcium concentration seems to stabilize around 0.020M. Overall, the observations witnesses of a calcium production from the chalk core. Also magnesium is detected in the effluent after one day of flooding with the new brine, but the concentration does not manage to reach the original of 0.219M found in the injected brine. This indicates an opposite effect compared to the one observed for calcium, as some magnesium is retained within the chalk core. By adding the total magnesium present in the effluent with the production of calcium, the value eventually starts to fluctuate around the original concentration of 0.219M.

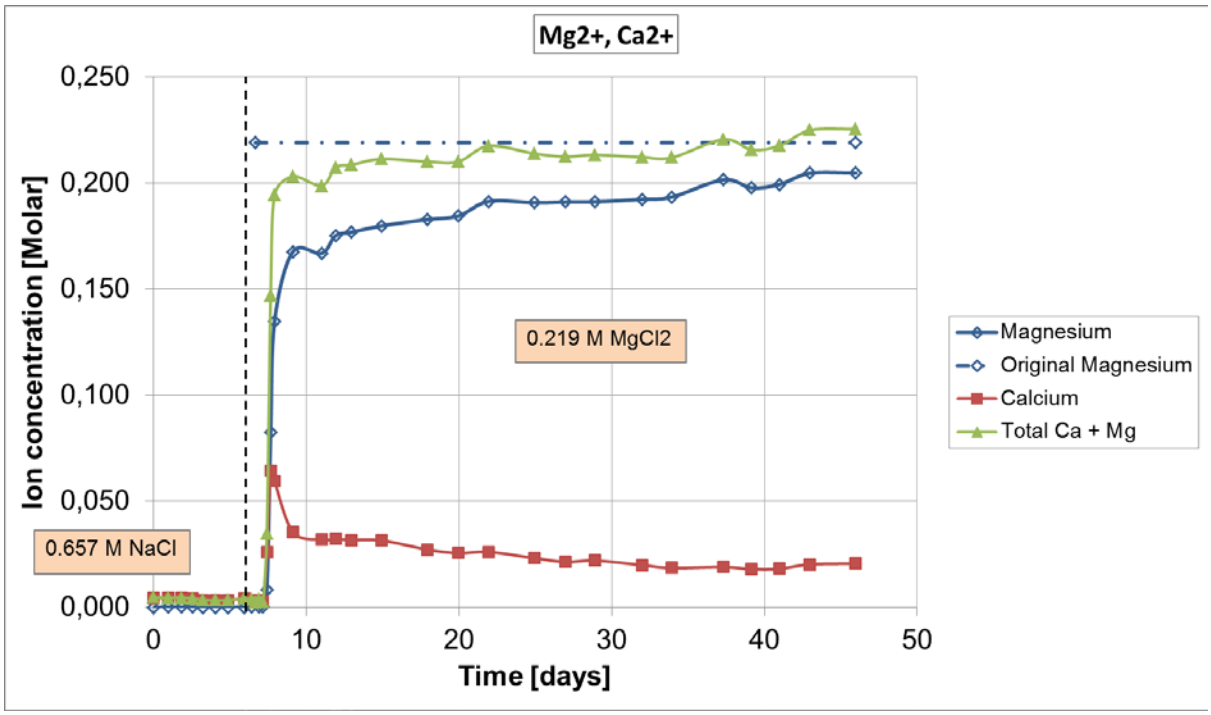

Figure 4.17: Ion concentration present in the effluent brine plotted as a function of time for OB SV 6. Magnesium and calcium ions and their original concentrations.

4.2.3 Porosity measurements

The porosity measurements were based on values obtained prior to and after testing (see calculations in section 3.6). The mechanical method to measure the porosity only considers a potential change in the bulk volume of the core, whereas the chemical method includes chemical alterations of the grains inflicted by the chalk-water interactions.

By studying the measured values of OB SV 9 flooded with SSW, it can be seen that the core has experienced a small reduction in density in addition to a lower porosity value. OB SV 6 on the other hand, has increased its density after testing compared to prior, but the porosity value is lower as for OB SV 12 (see table 4.13).

Core Sample	V_B [CC]		ε_v	M_s [g]		ρ[g/cc]		ϕ [%]			
								B		A	
	B	A		B	A	B	A	M	M+C	M	M+C
OB SV 9 (SSW)	80	75.4	0.0575	126.57	127.26	2.69	2.67	41.34	41.34	37.76	37.02
OB SV 6 ($MgCl_2$)	79.8	75.6	0.052	126.65	126.28	2.68	2.72	40.81	40.81	37.55	38.6

Table 4.13: Porosity values for OB SV 9 and OB SV 6

5 Discussion

5.1 Hydrostatic loading analysis

All the cores were extracted from the same outcrop and Mons chalk block to have the same basis of comparison for the experimental results. However, the porosity varies somewhat for the different cores as a result of small changes within the block itself. All the cores were flooded with 0.657M NaCl during the hydrostatic phase but some cores were fractured whereas other remained intact (see table 5.1).

Although, for hydrostatic loading, the fractures does not seem to have a significant impact on the axial deformation as might expected due to less matrix for core support during loading. OB SV 12 has somewhat higher axial strain, but OB SV 4 and OB SV 18 (also fractured) show similar strengths compared to the intact cores.

As mentioned earlier, they show similar behavior when regarding the axial strain under the same amount of stress applied. However, there are some minor variations as OB SV 9 and OB SV 12 tend to deviate somewhat from the other cores at the end of the linear trend, hence reflecting a slightly less mechanical weakness. As seen in table 5.1, OB SV 9 and OB SV 12 have the highest porosities with an equal value of 41.34%, and it is a known fact that the mechanical strength of chalk decreases as the porosity increases(DaSilva, 1985). This observation can be supported by looking at the total axial strain for the mentioned core samples, as they have the highest values of 1.07% and 0.90%, respectively. When studying the yield strength for the various cores they all have quite similar values varying from 9.1 MPa - 9.9 MPa, but again, OB SV 12 and OB SV 9 tend to deform faster (lower yield) may due to a somewhat higher porosity. Yet, OB SV 18 and OB SV 12 have equal yield strengths, but the axial strain in the same particular point is larger for the latter with 0.57% compared to 0.47% of OB SV 18. This is reflected by the values of K-modulus which shows that OB SV 18 has a higher stiffness (K=0.753 GPa) compared to core OB SV 12 (K=0.625 GPa).

Overall, by comparing the porosity and yield strength for the different cores they show relatively similar values. This observation supports the in-house experience, that cores drilled in the same direction from one and the same chalk block have approximately the same porosities, as well as small variations in yield strength during hydrostatic tests (Korsnes, Wersland, Austad, & Madland, 2008). Also the bulk modulus having such close values contributes to the reasoning. Experiments carried out by (Korsnes et al., 2008) showed that the drilling direction, either vertical or horizontal, from the same exact chalk block had a huge impact on the mechanical properties. The studies were performed on Liege and Stevns Klint outcrop chalks with similar results, but the number of tests were substantially higher for the latter (9 versus 2 tests), hence the observations could only be based from the Stevns Klint samples. The test results showed that the average axial yield stress for Stevns Klint samples drilled in vertical and horizontal directions were 6.26 and 8.12

MPa, which is a major difference. For the bulk modulus the average values for vertical and horizontal direction was 0.78 GPa and 1.14 GPa, respectively. In the experimental work carried out by (Veen, 2012) this differences was clearly visible when comparing the mechanical strength of similar outcrop chalk. Three Liege cores originated from the same outcrop, but they were not drilled out from the same block and since the blocks are unmarked with bedding direction this could result in one core being drilled out vertically whereas the other one horizontally. Two of the cores that were extracted from the same chalk block turned out to have quite similar bulk and yield values, whilst the last core from a different chalk block had a magnitude of 1.60 and 1.51 smaller for the bulk modulus and a factor of 0.94 smaller for the yield strength. With this said, by having test material that are highly comparable as for these experiments, will make it easier to differentiate the impact of the fractures and different flooding brines.

Chalk core	**Fractured/ Intact core sample**	**Porosity**	**Flooding brine**	**Yield strength**	**Bulk modulus**	**Axial strain at yield point**	**Total axial strain after hydrostatic loading**
OB SV 12	Fracture	41.34 %	0.657 M NaCl	9.4 MPa	0.625 GPa	0.57%	1.07 %
OB SV 4		40.49 %	0.657 M NaCl	9.6 MPa	0.750 GPa	0.48%	0.81 %
OB SV 18		41.18 %	0.657 M NaCl	9.4 MPa	0.753 GPa	0.47%	0.84 %
OB SV 9	Intact	41.34 %	0.657 M NaCl	9.1 MPa	0.696 GPa	0.47%	0.90%
OB SV 6		40.81%	0.657 M NaCl	9.9 MPa	0.685 GPa	0.53%	0.81%

Table 5.1: Obtained values for the hydrostatic loading for all the cores

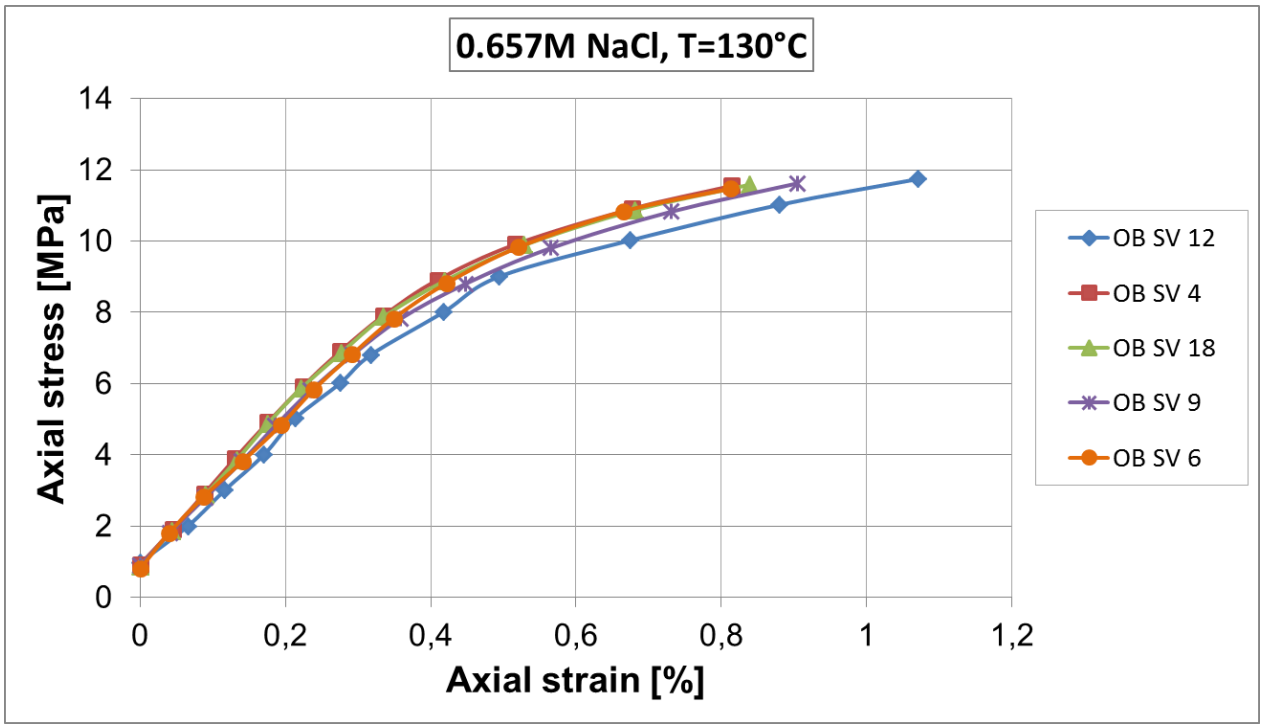

Figure 5.1: Axial stress [MPa] plotted as a function of axial strain [%] for all the core samples.

5.2 Creep phase analysis

When the axial creep strains of all the cores are compared, it is obvious that both the fracture in the core and the different brines interfere and weakens the chalk in distinctive ways.

5.2.1 The effect of fractures with regards to creep

The creep curves show different behaviors when flooded with SSW and 0.219M $MgCl_2$ and the fractures tend to have a clear impact. The observations are summarized in the following section:

Both OB SV 6 (intact) and OB SV 4 (fractured) were flooded with 0.219M $MgCl_2$. The two cores show relatively similar behavior when flooded with 0.657M NaCl, as the axial creep strain reduces and tends to develop into a transient phase (see Fig. 5.2). Yet, OB SV 4 (fractured) deforms slightly more than OB SV 6 (intact) with axial creep strains of 1.25% and 1.15% just prior to brine change. When the brine is changed to 0.219M $MgCl_2$, OB SV 4 (fractured) experiences a reduction in the strain rate whereas the strain rate of OB SV 6 (intact) accelerates. The response of OB SV 4 is most likely caused by the fracture in the core sample, as the flooding brine will tend to follow the easiest path through the hole and hence use longer time to diffuse into the matrix. For OB SV 6 on the other hand, larger parts of the matrix will be contacted in a much faster pace as the core is intact. In this way, the chalk-water interaction will start to deform the grain structure immediately while the process will be “delayed” for the fractured core sample. It should however be noted that after

approximately 20 days of creep time the two cores achieves fairly similar creep rates (see Fig.5.2):

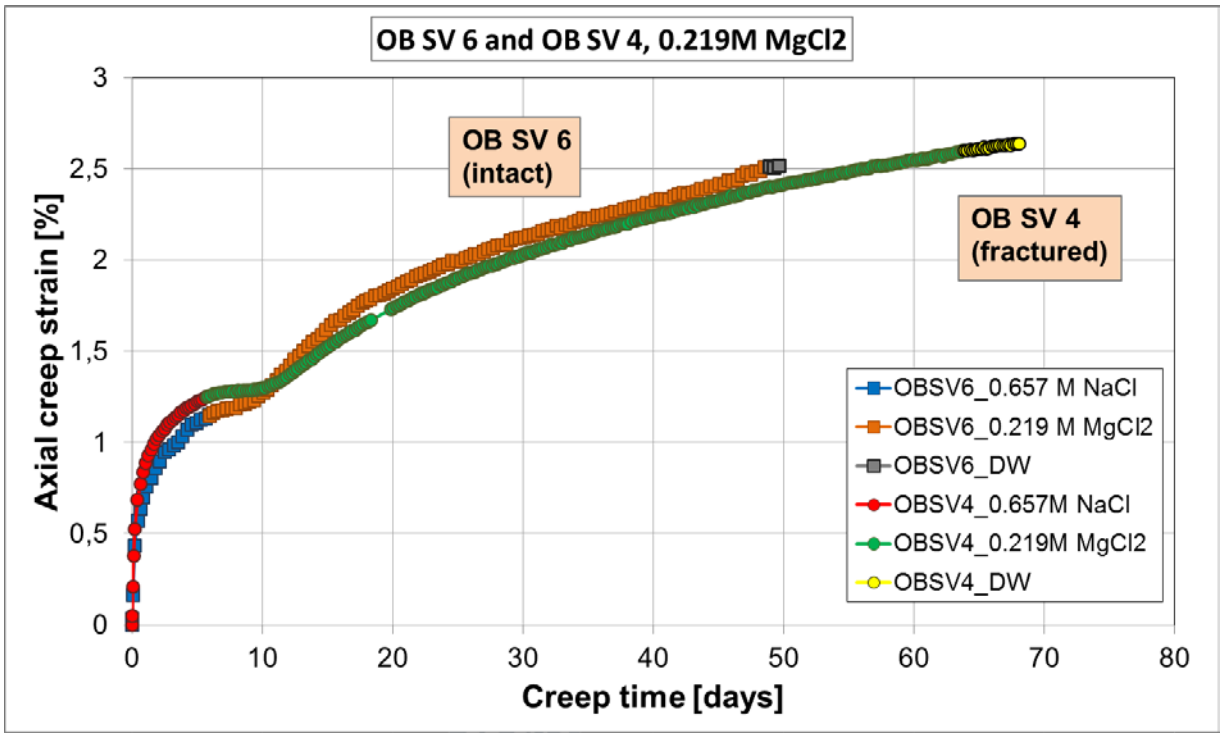

Figure 5.2: Axial creep strain [%] plotted as a function of creep time [days] for OB SV 6 and OB SV 4, both flooded with 0.219 M $MgCl_2$.

Both OB SV 12 (fractured) and OB SV 9 (intact) were flooded with synthetic seawater (SSW). The two cores show quite distinct behavior when flooded with 0.657M NaCl, where OB SV 9 has an axial strain of 1.05% prior to brine change while OB SV 12 has a value of 1.59%. This can be a result of the fracture within OB SV 12 since less matrix supports the core and hence make it more fragile. However, when the brine is substituted with SSW, the strain rate of OB SV 12 (fractured) decreases while the strain rate of OB SV 9 (intact) accelerates rapidly. The two cores witness of a relatively similar development in the creep strain, when compared with the previous case of OB SV 6 and OB SV 4 (see Fig.5.2). Again, it seems like the SSW follow the fracture within OB SV 12 and thus spend longer time to reach the rest of the matrix – hence the creep rate will be reduced. For OB SV 9 (intact) on the other hand, the grain structure will be soaked by the fluid in a much larger extent right from the start, and the deformation process occurs faster. By studying OB SV 9 in Fig.5.3, it can be seen that the creep phase stops rather abruptly after only 21 days of flooding. It turned out from the differential pressure readings in addition to lack of effluent water from the core, that the plug was clogged (see Fig. 5.4):

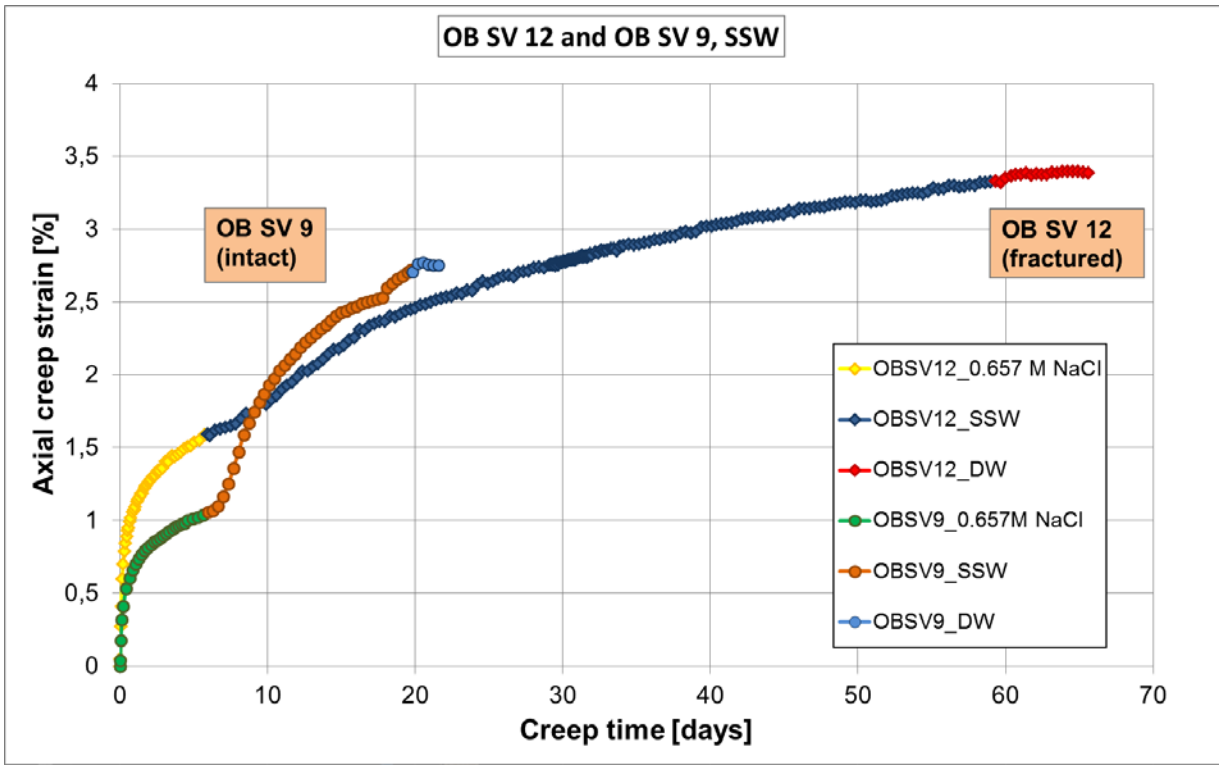

Figure 5.3: Axial creep strain [%] plotted as a function of creep time [days] for OB SV 12 and OB SV 9, both flooded with SSW.

From figure 5.4, it can look like the core sample starts to get clogged after approximately 14 days as the differential pressure (ΔP), starts to increase sharply and thereby causes the effective stresses to decrease. Next, the bypass was opened, the differential pressure dropped and the effective stresses increased again. This transition into a new accelerating creep strain can clearly be seen after 18 days. The effect of flooding with SSW on intact chalk cores was also examined by (Haddadi, 2013), although the chalk was of a mechanically stronger type (Kansas). The core was first flooded with 1.833M NaCl and later had the brine substituted with SSW of equal composition used in this thesis. However, (Haddadi, 2013) did not experience any remarkable change in creep rate during the course of time, neither any plugging of the core.

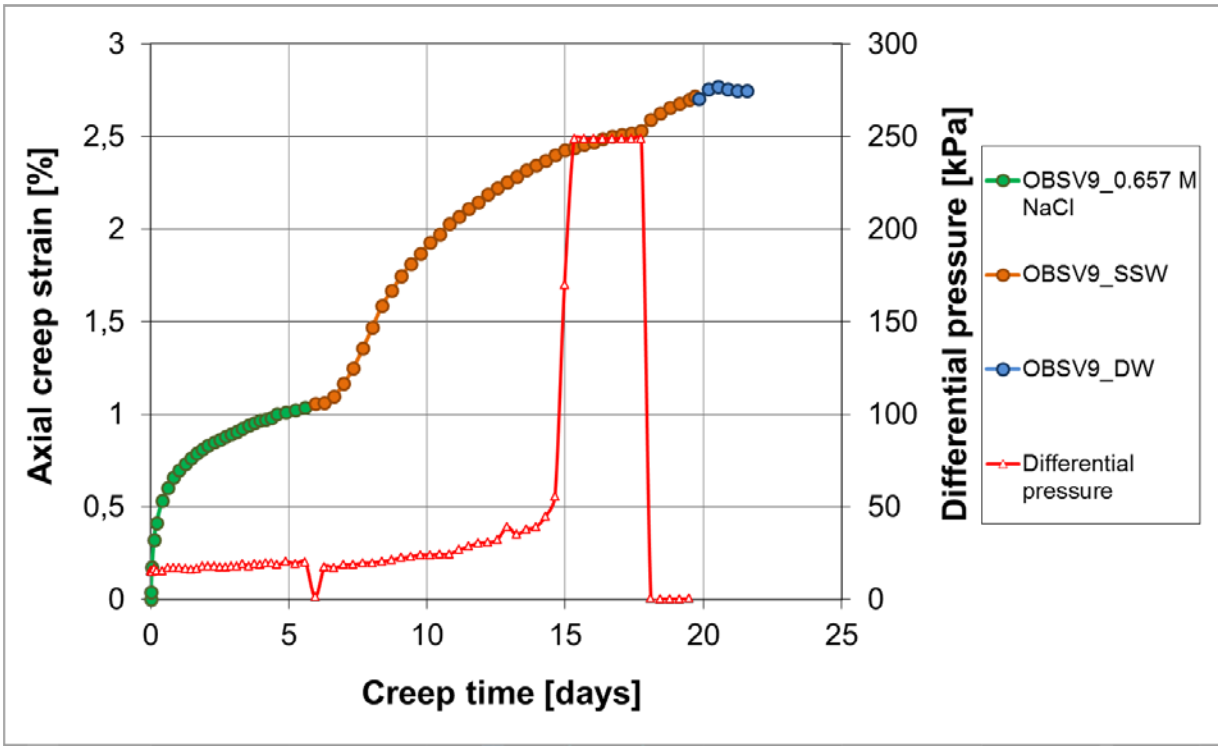

Figure 5.4: Axial creep strain [%] plotted as a function of creep time [days] for OB SV 9. The red line illustrates the differential pressure that occurred as a result of the core plug being clogged.

5.2.2 The effect of flooding fluid with regards to creep

To observe the effect of the flooding fluids and how they influence the chalk differently with regards to creep, the fractured cores are first plotted together - followed by the intact core samples. One graph illustrates axial creep strain [%] as a function of creep time [days] whereas a second graph includes the ion concentration in addition to the creep curve.

Fractured core samples flooded with SSW and 0.219M $MgCl_2$

To get a better overview, all the fractured core samples are plotted together in figure 5.5, but it should be noted that the cores are flooded with different types of brines. By looking at OB SV 18 flooded solely by 0.657M NaCl, the axial creep strain reduces during the course of time and the curve tends to develop into a transient creep pattern. This core sample was included in the experimental results with the intention of using it as a reference. In this way, the effect of flooding fluid on the mechanical strength of chalk is clearly visible. By comparing OB SV 12 and OB SV 4 during the first stage of creep (prior to brine change), they both were flooded with 0.657M NaCl. OB SV 12 is somewhat more deformed than OB SV 4 with axial creep strains of 1.59% and 1.25% just before the new brines are introduced. OB SV 12 and OB SV 4 show quite distinct strain rates when the flooding brines are changed; for OB SV 4 flooded with 0.219M $MgCl_2$ the strain rate is substantially lower than for OB SV 12 flooded with SSW. OB SV 12 deforms the most with a total axial creep strain of 3.38%

whereas OB SV 4 reaches a value of 2.63% (see Fig 5.5). To get a further understanding and to explain the different behavior of the chalk cores, it is necessary to analyze the ion concentrations in the respective brines used for flooding. Each creep curve will therefore be illustrated separately in the following section, plotted together with the ion concentration found in the effluent water.

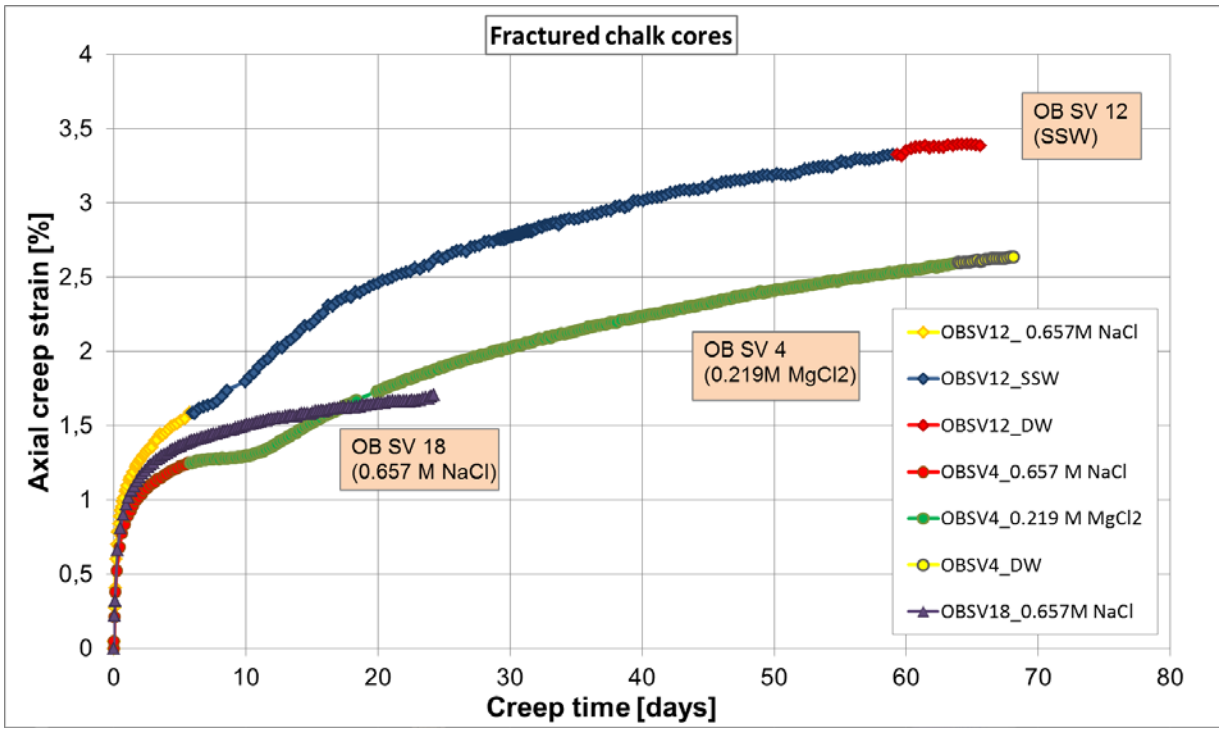

Figure 5.5: Axial creep strain [%] plotted as a function of creep time [days] for OB SV 12, OB SV 4 and OB SV 18 - all *fractured* only flooded with different brines.

By looking closer at OB SV 12 flooded with SSW (see Fig. 5.6), it can be observed an increased concentration of magnesium and calcium in the effluent as the brine is changed from 0.647M NaCl to SSW. However, the magnesium concentration tends to stabilize at a value slightly under the original of 0.045M Mg2+ present in the seawater. This is a very interesting observation as it indicates that some magnesium is left within the core, even though it contains a hole. One might expected that the magnesium concentration would reach its original, as the water follows the easiest path (hole) and only causes minor interaction with the surrounding matrix. When looking at the creep curve, it can be seen that the axial creep strain starts to accelerate when SSW is injected as magnesium ions are lost and calcium produced (see Fig 5.6). In (Madland et al., 2011) it was demonstrated that magnesium ions present in the SSW initiated precipitation of other minerals such as magnesium-bearing carbonates and silicates. “The precipitation of secondary minerals led to a net transport of calcium out of the core, which was interpreted as dissolution of calcite”. This reaction would in turn influence the rate of deformation, clearly visible from the creep curve. It should also be noted that sulfate more or less reached its original value during the flooding, so any deformation inflicted by the presence of sulfate ions is probably unlikely.

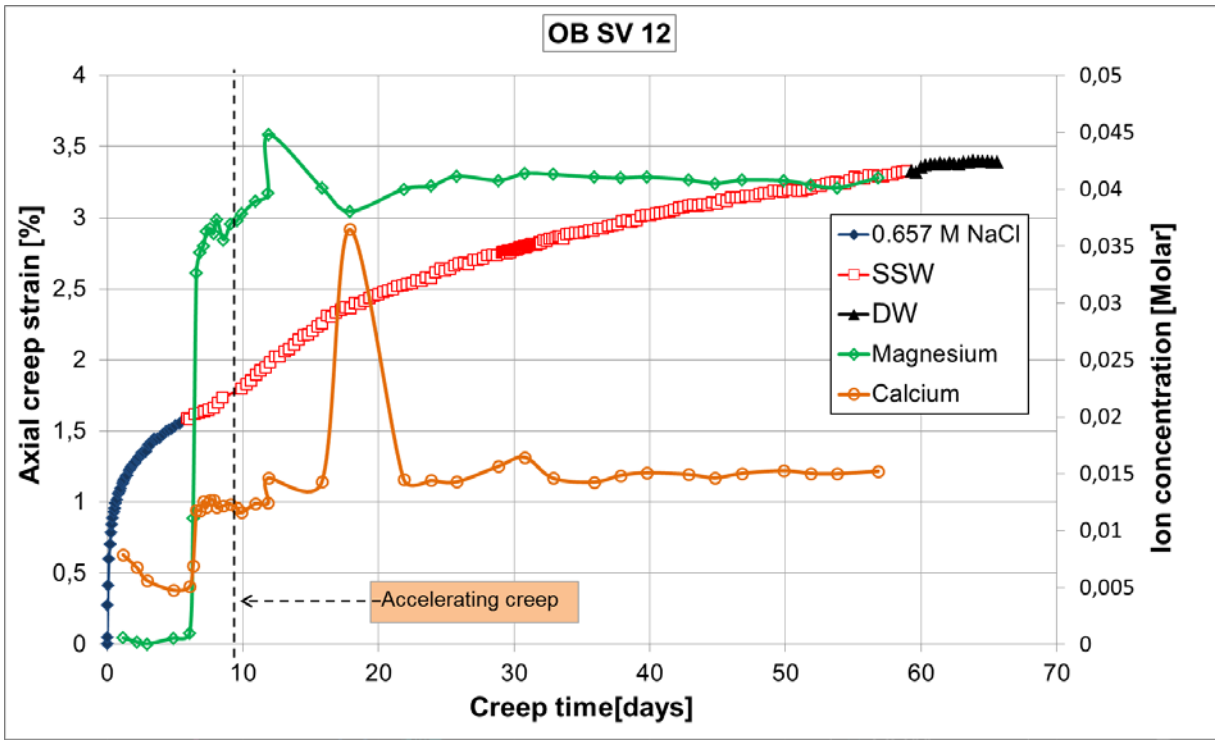

Figure 5.6: Axial creep strain [%] plotted as a function of creep time [days] in addition to ion concentration [molar] for OB SV 12 (fractured).

By looking closer at OB SV 4 flooded with 0.219M $MgCl_2$ (see Fig. 5.7), there is noted a high concentration of magnesium ions in the effluent almost immediately after $MgCl_2$ is introduced. However, the concentration never reaches the original value of 0.219M, which indicates retention of magnesium ions within the core. So also for this case, it appears that a substitution process occurs despite of the hole. In addition to the loss of magnesium, a small amount of calcium ions are being produced when the flooding brine is changed. What is interesting to notice is that it seems to be a dependency of increased concentrations of the respective ions in the same particular point where the accelerating creep phase is initiated. Other experiments carried out by (Madland et al., 2011) on high porosity outcrop chalks of Liege and Stevns Klint, show a significant loss of magnesium and additional amount of calcium detected in the effluent when flooded with MgCl2 - independent of the chalk type tested. Also the fact that the magnesium ions are smaller than calcium ions, supports the observation of increased compaction rate during the substitution process (Madland et al., 2011) See figure 5.7:

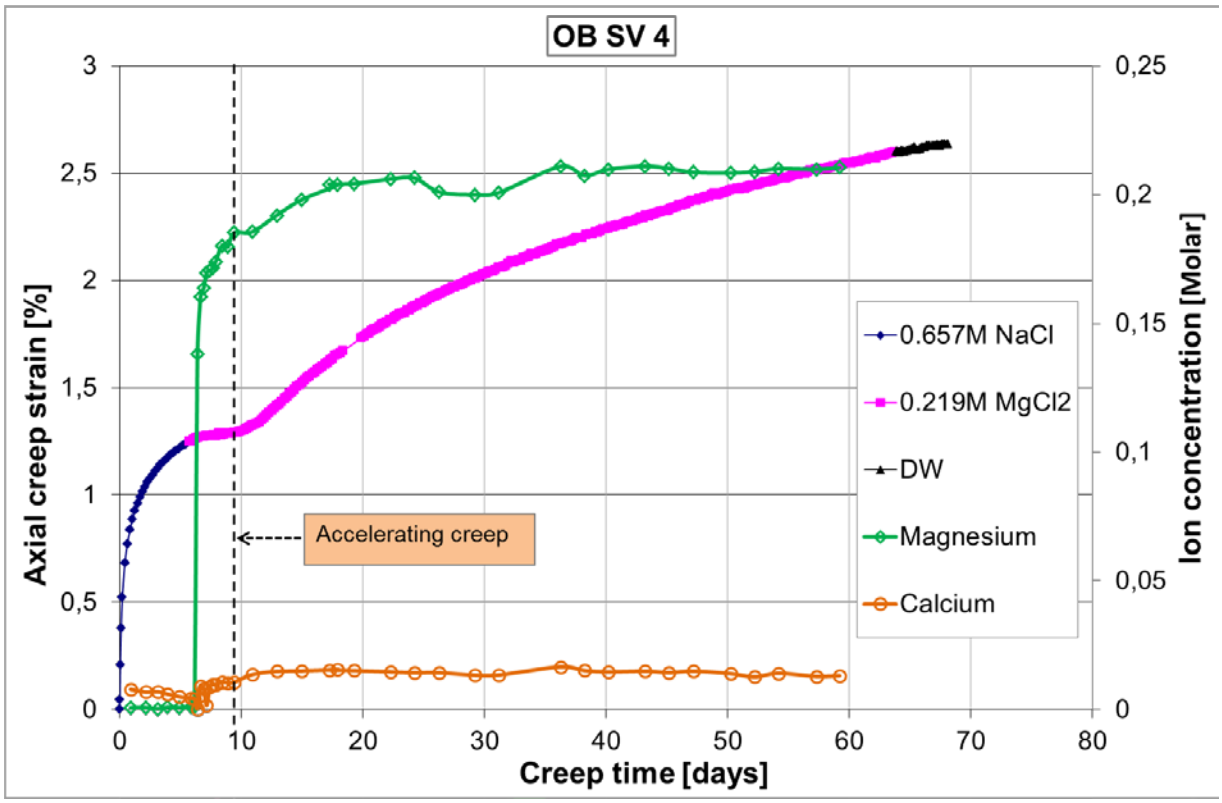

Figure 5.7: Axial creep strain [%] plotted as a function of creep time [days] in addition to ion concentration [molar] for OB SV 4 (fractured).

Intact core samples flooded with SSW and 0.219M $MgCl_2$

To get a better overview, the two intact core samples are plotted together in figure 5.8, but the cores are flooded with different types of brines. When flooded with 0.657M NaCl the cores experiences relatively similar strain rates and tends to develop into a transient creep phase. Although, the axial creep strain prior to brine change is slightly higher for OB SV 6 with 1.15%, and 1.05% for OB SV 9. By comparing the two cores, the creep curve develops rather differently when subjected to the new brine. OB SV 6 flooded with 0.219M $MgCl_2$ have a much lower strain rate compared to OB SV 9 flooded with SSW. However, the total axial creep strain is not that different with OB SV 9 ending at a total value of 2.74% whereas OB SV 6 reaches a value of 2.51%. Also for this case, to get a further understanding and to explain the different behavior of the chalk cores, it is necessary to analyze the ion concentrations in the respective brines used for flooding. Each creep curve will therefore be illustrated separately in the following section, plotted together with the ion concentration found in the effluent water.

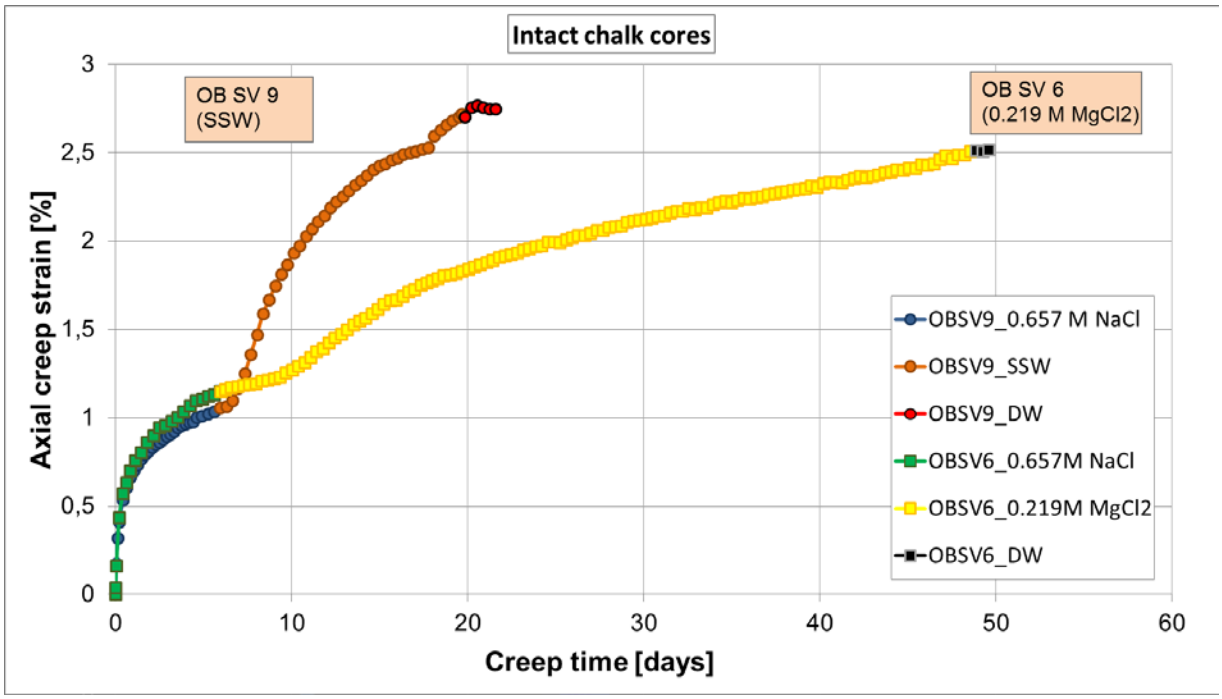

Figure 5.8: Axial creep strain [%] plotted as a function of creep time [days] for OB SV 9 and OB SV 6 - both intact only flooded with different brines.

By looking closer at OB SV 6 flooded with 0.219M $MgCl_2$ (see Fig. 5.9), it can be observed that the magnesium concentration is rapidly increasing at the same time as calcium is being produced. However, the magnesium concentration never reaches the original value of 0.219M which indicates a loss of magnesium ions within the core. This outcome was expected because of the core being intact, as numerous experiments during the last years have experienced similar results. Tests performed by (Madland et al., 2011) clearly show the effect of magnesium ions when regarding the substitution and precipitation process. This effect of magnesium can be observed in figure 5.9 as the accelerating creep (dotted line) coincides with an increased concentration of magnesium - and thereby a reduction of calcium ions found in the effluent. During the course of time, the concentrations tend to develop in a similar pattern which indicates an establishment of equilibrium between magnesium and calcium in the chalk. These combined observations of magnesium loss and calcium production with an accelerating creep compaction, can witness of precipitation of secondary magnesium bearing minerals as a direct result of the chalk being dissolved (see figure 5.9).

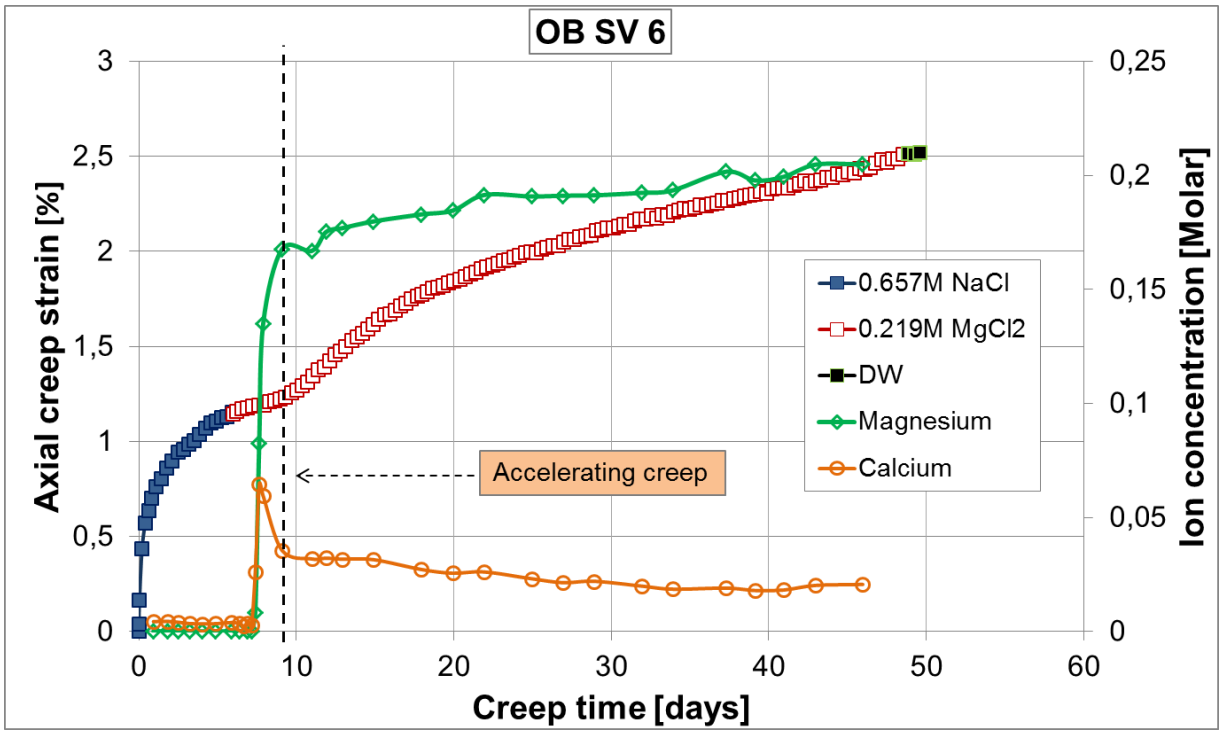

Figure 5.9: Axial creep strain [%] plotted as a function of creep time [days] in addition to ion concentration [molar] for OB SV 6 (intact).

By looking at OB SV 9 (see Fig. 5.10) it can be seen that the core experiences a rapid deformation when the flooding brine is changed to SSW. Short time after, there is detected a magnesium concentration in the effluent combined with a production of calcium ions. The creep rate evolves very quickly, as the SSW tends to intrude the matrix immediately and weaken the chalk grains. After approximately 14 days of flooding the differential pressure increased as a result of the core being clogged (see Fig 5.4). Tests carried out by (Heggheim, Madland, Risnes, & Austad, 2005) showed remarkable similarities with an incidence of clogging when flooding with SSW. The author suggested that when sulfate was reduced in the injected brine in addition to clogging, the observations pointed towards precipitation of anhydrite ($CaSO_4$) within the core. This assumption was supported upon the fact of a lower total Mg^{2+} and Ca^{2+} concentration present in the effluent, compared to the original Mg^{2+} concentration prior to brine change. In the case of OB SV 9 the chemical analysis actually proved a decreased concentration of sulfate in the effluent, and the original concentration was never reached. Also here, the total Mg^{2+} and Ca^{2+} concentration fluctuated around a value somewhat lower than that of the original Mg^{2+}. This observations seen in perspective with the experimental results of (Heggheim et al., 2005) ,can indicate a possible precipitation of anhydrite in the chalk core (see figure 5.10). For further comparison, it can be worth to mentioned a tests carried out by (Haddadi, 2013) performed on Kansas chalk. The core sample was flooded with SSW of same concentration used in these experiments, but as mentioned earlier; the core experienced just a minor change in the creep. When the effluent water then was analyzed, the injected brine did not show any loss of sulfate ions within the core sample, neither was the core plug clogged. These are interesting observations, as it

might seem like a reduction in sulfate concentration can contribute to precipitation of anhydrite, and hence clogging of the core. Recent studies carried out by (Megawati et al., 2012) also witnessed a weakening effect induced by sulfate present in the flooding brine. The experiments showed that when sulfate was adsorbed by the pore water, the core surface got negatively charged which in turn resulted in a disjoining pressure between the grains. Because of the forces that arise, the mechanical strength of the chalk was reduced and thus the strain rates increased.

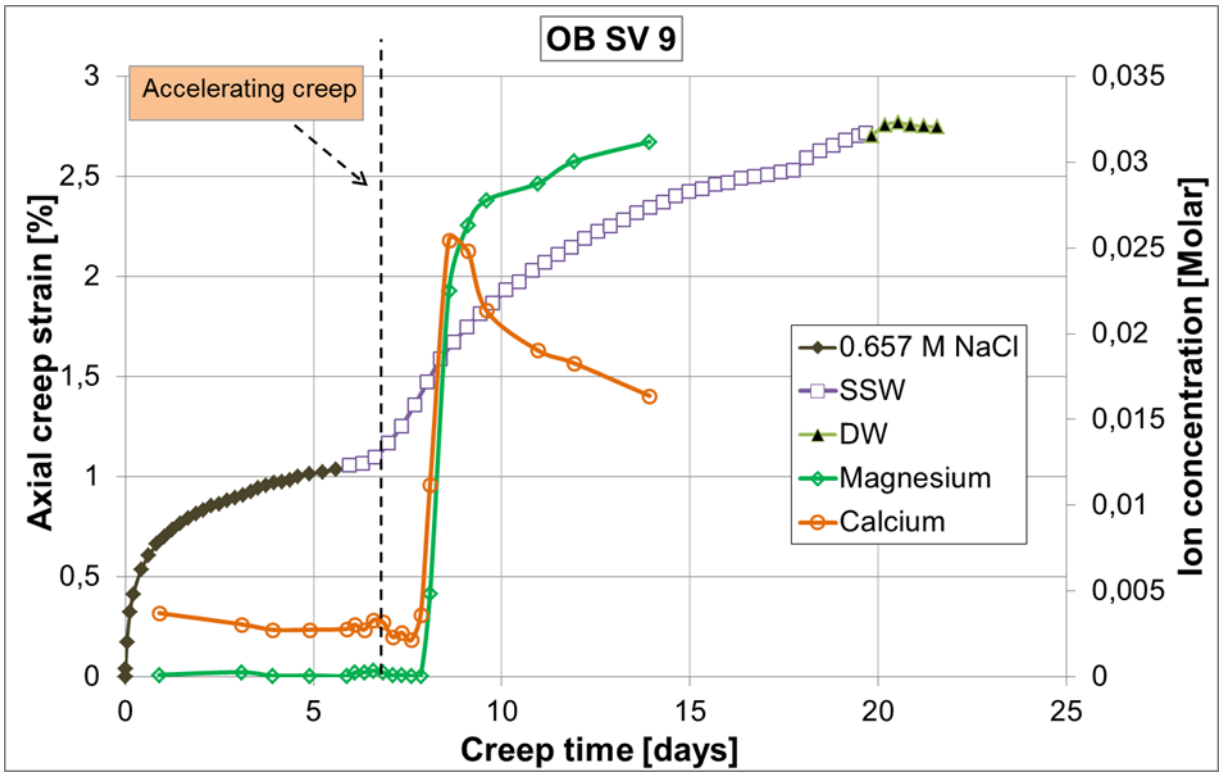

Figure 5.10: Axial creep strain [%] plotted as a function of creep time [days] in addition to ion concentration [molar] for OB SV 9 (intact).

5.3 SEM image of a fractured core sample

A core slice from OB SV 12 flooded with SSW, was studied by using a scanning electron microscopy (SEM-EDS) with X-ray microanalysis. The intention was to detect potential precipitations of new minerals within the chalk core and observe to which extent the matrix was affected by the flooding brine. Since the core contained an induced fracture, it was of interest to study directly inside the hole and compare with images from further out into the exterior.

The first image is from directly inside the hole, and it is clear that the chalk appears to be altered as coccoliths are undetectable in addition to unclean calcite (see Fig. 5.11).

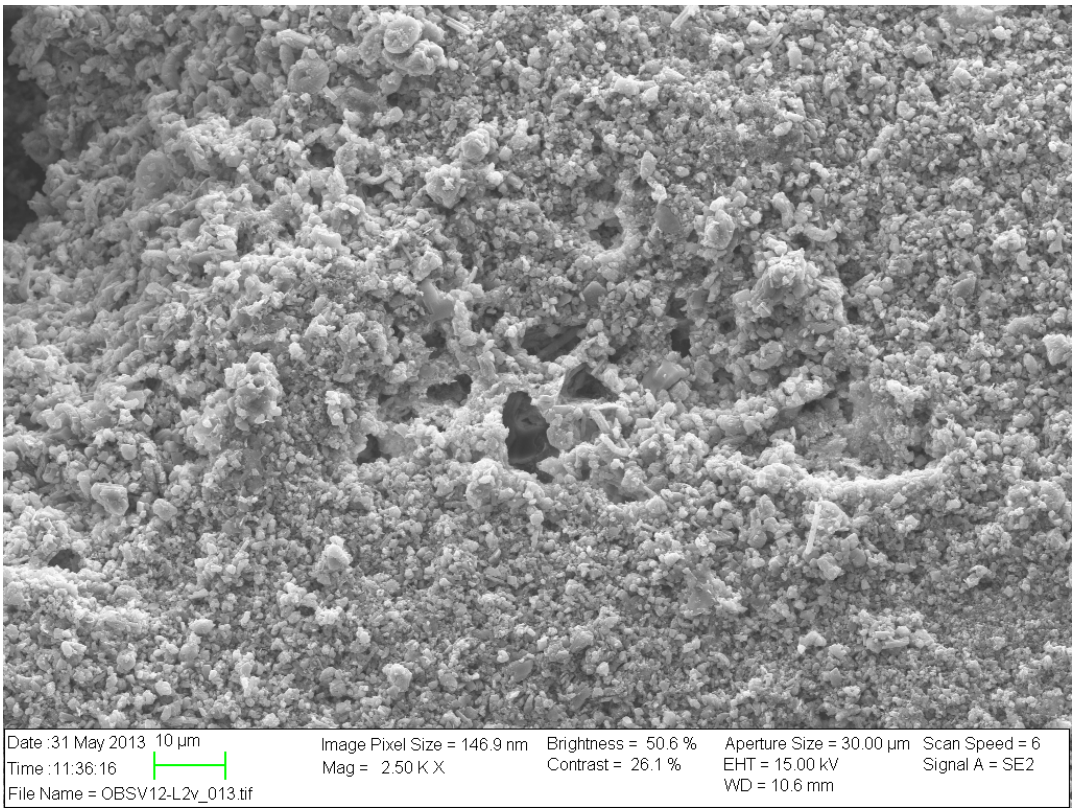

Figure 5.11: SEM micrograph of the chalk core OB SV 12 after flooding with SSW. This image is from directly inside the hole, and the chalk surface appears to be altered by the fluid. Notice that no coccolith rings can be detected and that the calcite looks considerably unclean.

Figure 5.12 shows just outside the hole. In this image, it is now possible to detect coccolith rings and the surface appears to be much cleaner.

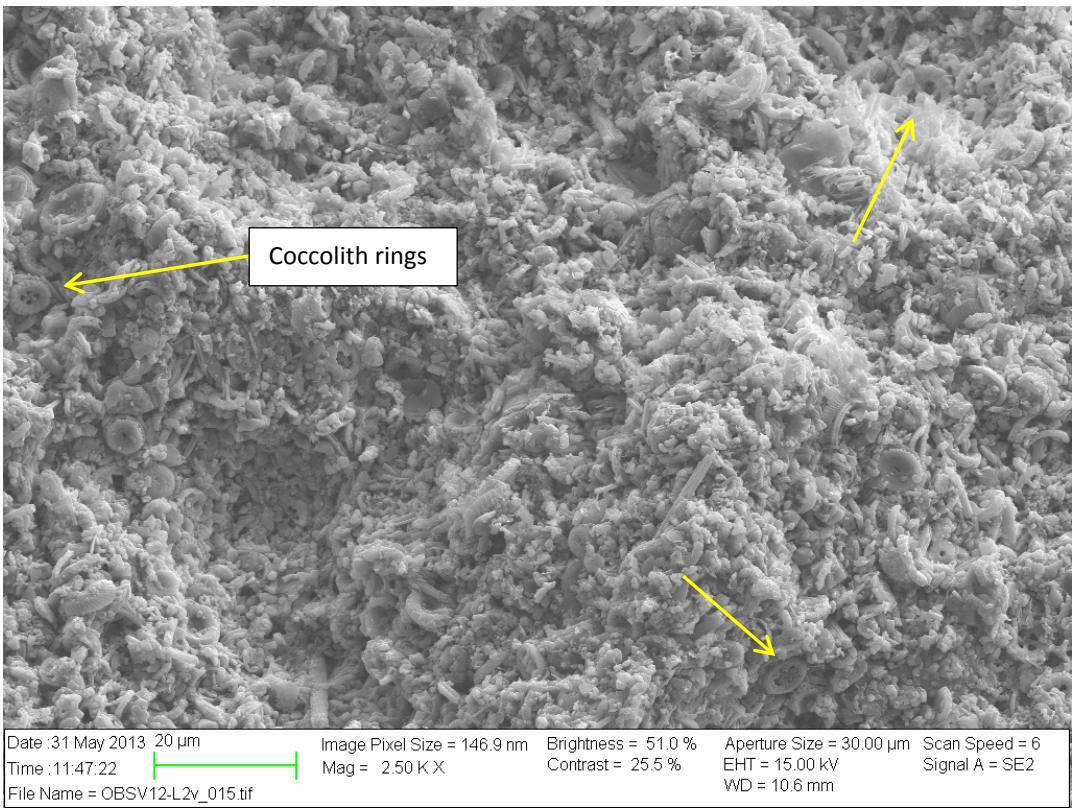

Figure 5.12: SEM micrograph of the chalk core OB SV 12 after flooding with SSW. This image shows the outside of the hole, and coccolith rings can already be detected even though the surface still is clearly affected by the SSW.

Figure 5.13 is showing the grains close to the exterior of the core, and now even more coccolith rings can be observed due to a cleaner surface. It appears that the injected brine have not interacted with the outer matrix, in such a great extent as within the fracture region.

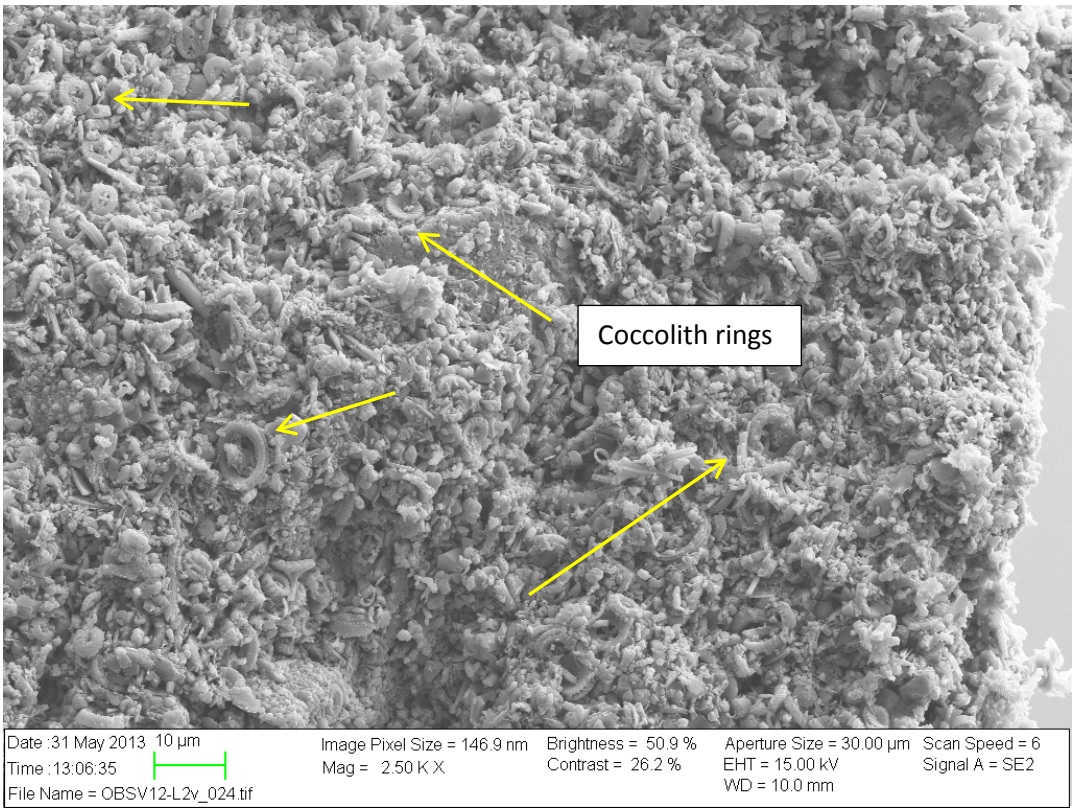

Figure 5.13: SEM micrograph of the chalk core OB SV 12 after flooding with SSW. The image is from the exterior of the core, and the surface looks a lot cleaner as more coccolith rings can be spotted.

The next image is provided from another slice of the same core, but it is included as it shows some clay-like minerals covering the grains inside the hole's wall (see Fig. 5.14).

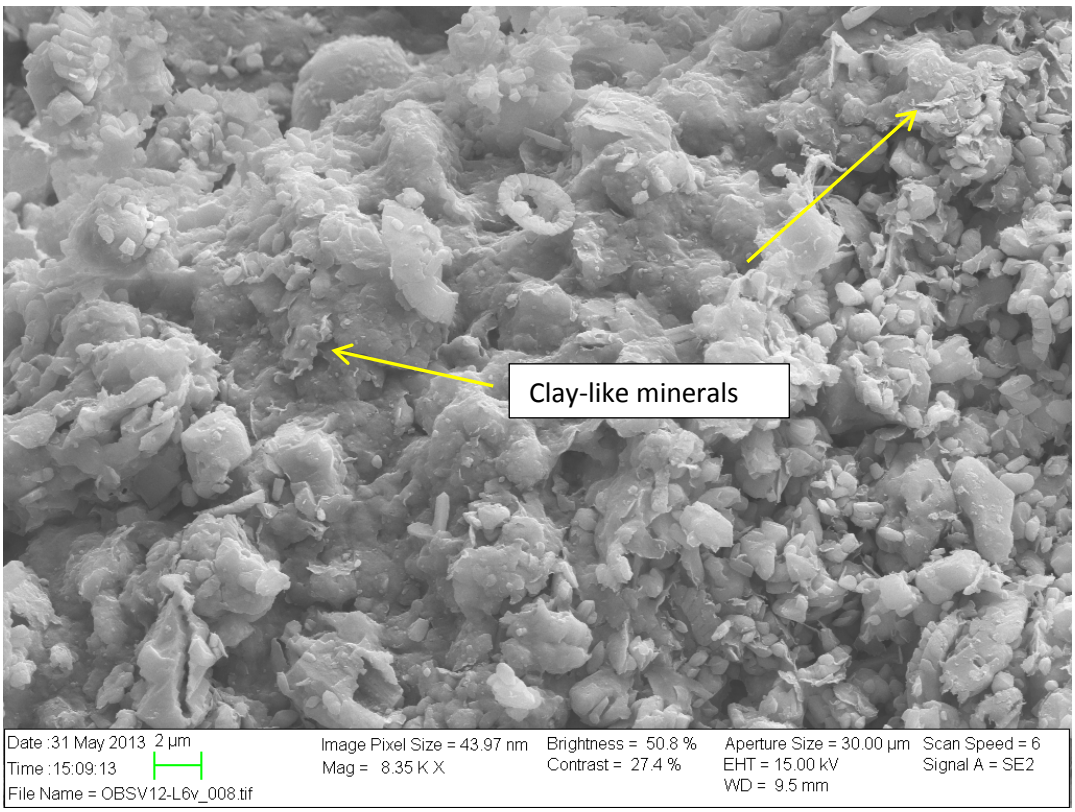

Figure 5.14: SEM micrograph of the chalk core OB SV 12 after flooding with SSW. Calcite grains covered with clay like minerals (silicates?).

The graph illustrates the amount of magnesium ions [weight %] precipitated within the chalk core, from the hole's wall to the outer exterior (see Fig.5.15). It can be seen that the concentration is very high directly in the hole, but tend to decrease further out in the exterior of the matrix.

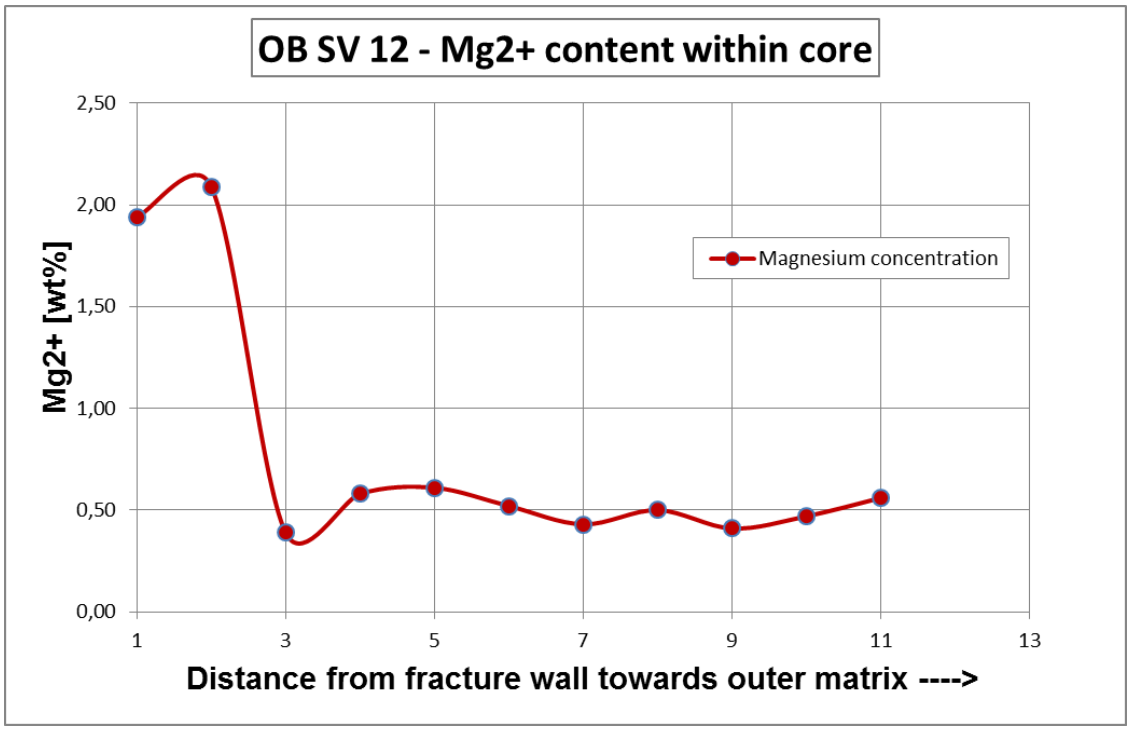

6 Conclusion

The effect of fractures and different flooding brines on the mechanical properties of chalk, has been demonstrated during hydrostatic loading and time-dependent creep tests. SEM images provided from one of the fractured core samples made it possible to detect precipitated minerals within the hole itself, and to further localize the areas affected by the injected fluid. The overall observations of chalks mechanical behavior in addition to these SEM images, coincided well with the chemical analysis of ions present in the effluent.

It is observed that the cores did not experience any clear differences in mechanical strength during the hydrostatic loading phase, were all cores were flooded with 0.657M NaCl. The small differences that occurred however, are most likely caused by variations in porosity values rather than the fractures. This conclusion were based on the two cores having equal and additionally the highest porosities, where one core was fractured and the other one intact; it turned out that both cores also achieved the lowest yield points and highest total axial deformation. The remaining cores with the lowest porosities on the other hand experienced the highest yield point and lowest total axial deformation, also being one intact and one fractured core.

During the first 6 days of creep when flooding with 0.657M NaCl, all the cores showed similar behaviors with a reduction in strain rate and thereby a transition into transient (primary) creep phase. There was however a somewhat higher deformation for the fractured cores compared to the intact, just prior to brine substitution. This minor difference in mechanical strength was expected to occur since the fractured core samples have less matrix to support the core during loading.

By comparing all the cores during creep phase, the observations can be summarized as follows: The two cores flooded with SSW experienced the highest deformation rates in addition to highest total axial strains after creep phase – even though one core had a fracture whereas the other one was intact. However, when analyzing these further, the intact core had a higher strain rate as a result of the matrix being immediately affected by the injected brine and the core was later clogged. The other cores flooded with 0.219M $MgCl_2$ experienced similar behaviors, as the intact core had a slightly higher deformation rate compared to the fractured core sample. Although for this case, the rates became almost equal after approximately 20 days of flooding. The one core having the higher rate, is assumed to have the same explanation of immediate invasion of flooding brine - and thus a faster deformation. To sum up; the cores that contained fractures deformed in a slower pace compared to core samples with intact matrix.

Chemical analysis of the cores effluent have shown that magnesium is lost within the core in addition to calcium production, both for the fractured and intact cores when flooded with SSW and 0.219M $MgCl_2$. However, for the fractured cores the magnesium concentration was closer to the original value as less ions was retained within the core due to the fracture itself. Effluent analysis from the intact core that was clogged, showed that a substantial amount of magnesium was left within the core in addition to sulfate. It was suggested that the high creep rate and the resulting clogging were caused by the presence of sulfate ions and precipitation of secondary minerals like anhydrite. For the case of the fractured core flooded with SSW there was not observed any remarkable loss of sulfate, and the creep rate was hence lower.

SEM (scanning electron microscope) images from the fractured core flooded with SSW, revealed that the hole's walls was severely damaged by the flooding fluid as no coccolith rings could be detected. Images from further out in the exterior on the other hand, showed a considerably cleaner grain structure. Another SEM image provided from a different part of the core, also affirmed evidence of clay-like minerals that was formed directly on the fracture walls.

7 Future work

In this experimental work, Mons chalk cores were flooded with SSW and 0.219 $MgCl_2$. A hole of 2 mm in diameter was drilled thought the matrix of some cores, whereas other remained intact. In this way it was possible to compare the effect of fractures with respect of creep, in addition to the influence of the different brines. The flooding rate used for these experiments was very low (0.022-0-023 PV/day), which can give the brines longer time to react with the chalk matrix and hence lead to increased deformation. To have a better basis of comparison it is proposed other factors to take into consideration for further work:

- Other types of outcrops
- Various flooding rates
- Various the size of the cylindrical hole (fracture)
- Natural made fractures by using uniaxial compressive tests

8 References

Abubeker, Elyas. (2013). *Water weakening of chalk -Comparison of intact and fractured cores.* Stavanger.

Austad, Tor, Strand, Skule, Madland, Merete V., Puntervold, Tina, & Korsnes, Reidar I. (2008). Seawater in Chalk: An EOR and Compaction Fluid. *SPE Reservoir Evaluation & Engineering, 11*(4), pp. 648-654. doi: 10.2118/118431-pa

Bjorlykke, Knut. (2010). Petroleum Geoscience : From Sedimentary Environments to Rock Physics / by Knut Bjorlykke (pp. 481): Berlin, Heidelberg : Springer-Verlag Berlin Heidelberg, 2010.

Bradl, H. B. (2005). Heavy metals in the environment : [origin, interaction and remediation] (pp. 4). Amsterdam; Boston: Elsevier Academic Press.

Butenuth, C., & De Freitas, M.H. (1989). Geomechanic abstract Properties of rock and soil Physico-chemical properties: Studies of the influence of water on calcite . Butenuth, C; De Freitas, M H Proc International Chalk Symposium, Brigton 4–7 September 1989P103–108. Publ London: Thomas Telford, 1990. *International Journal of Rock Mechanics and Mining Sciences and Geomechanics Abstracts, 28*, A145. doi: 10.1016/0148-9062(91)92819-K

DaSilva, F., Sarda, J.P., & Schroeder, C. (1985). Mechanical behavior of chalks. 2nd North Sea Chalk Symposium, Book 2. Stavanger, Norway.

Fjær, Erling, Holt, Rune M., Horsrud, Per, Raaen, Arne M., & Risnes, Rasmus (Eds.). (2008). *Petroleum related rock mechanics*. Amsterdam: Elsevier.

Fleet, Andrew J., Boldy, S. A. R., & Burley, S. D. (1999). Petroleum geology of Northwest Europe : proceedings of the 5th conference, held at the Barbican Centre, London, 26-29 October 1997 (pp. 1221 & 1224). London: Geological Society.

Gutierrez, M., Høeg, K., & Øino, L. E. (2000). The effect of fluid content on the mechanical behaviour of fractures in chalk. *Rock Mechanics and Rock Engineering, 33*(2), 93-117.

Haddadi, Diba. (2013). *An investigation of permeability and porosity evolution of Kansas chalk under in-situ conditions.* Stavanger.

Hardman, R. F. P. (1982). Chalk reservoirs of the North Sea. *Bulletin - Geological Society of Denmark, 30*, 119-137.

Heggheim, T., Madland, M. V., Risnes, R., & Austad, T. (2005). A chemical induced enhanced weakening of chalk by seawater. *Journal of Petroleum Science and Engineering, 46*(3), 171-184. doi: http://dx.doi.org/10.1016/j.petrol.2004.12.001

I.Trifu, Cezar. (2002). The mechanism of induced seismicity. In C. I.Trifu (Ed.), *Pageoph topical volumes* (pp. 405): Basel [u.a.] : Birkhäuser, 2002.

Korsnes, R. I., Wersland, E., Austad, T., & Madland, M. V. (2008). Anisotropy in chalk studied by rock mechanics. *Journal of Petroleum Science and Engineering, 62*(1-2), 28-35. doi: 10.1016/j.petrol.2008.06.004

Kvendseth, Stig S. (1988). Giant discovery : a history of Ekofisk through the first 20 years / Stig S. Kvendseth (pp. 199-202): Stavanger : Phillips Petroleum Company Norway, 1988.

Lawton, Rebecca Lawton Diana Panttaja Susan. (1997). Discover nature in the rocks : things to know and things to do (pp. 75-79). Mechanicsburg, PA: Stackpole Books.

Lucia, F. Jerry. (1999). *Carbonate reservoir characterization*. Berlin: Springer.

Madland, M. V., Hiorth, A., Omdal, E., Megawati, M., Hildebrand-Habel, T., Korsnes, R. I., . . . Cathles, L. M. (2011). Chemical Alterations Induced by Rock–Fluid Interactions When Injecting Brines in High Porosity Chalks. *Transport in Porous Media, 87*(3), 679-702. doi: 10.1007/s11242-010-9708-3

Megawati, M., Hiorth, A., & Madland, M. V. (2012). The Impact of Surface Charge on the Mechanical Behavior of High-Porosity Chalk. *Rock Mechanics and Rock Engineering*, 1-18. doi: 10.1007/s00603-012-0317-z

Michael J.Welch, Christine Souque, Viki Wood, Rob J.Knipe. (2013). Controls on fracture geometry in chalk.

Moore, C. H. (1989). Carbonate Diagenesis and Porosity (pp. 254). Burlington: Elsevier.

Nagel, N. B. (2001). Compaction and subsidence issues within the petroleum industry: From wilmington to ekofisk and beyond. *Physics and Chemistry of the Earth, Part A: Solid Earth and Geodesy, 26*(1–2), 3-14. doi: http://dx.doi.org/10.1016/S1464-1895(01)00015-1

Reidar, I. Korsnes, Merete, V. Madland, Tor, Austad, Stig, Haver, & Geir, Røsland. The effects of temperature on the water weakening of chalk by seawater. *Journal of Petroleum Science and Engineering, 60*, 183-193. doi: 10.1016/j.petrol.2007.06.001

Risnes, R. (2001). Deformation and yield in high porosity outcrop chalk. *Physics and Chemistry of the Earth, Part A: Solid Earth and Geodesy, 26*(1-2), 53-57. doi: 10.1016/S1464-1895(01)00022-9

Risnes, R., & Flaageng, O. (1999). Mechanical properties of chalk with emphasis on chalk-fluid interactions and micromechanical aspects. *Oil and Gas Science and Technology, 54*(6), 751-758.

Scholle, Peter A. (1977). Chalk diagenesis and its relation to petroleum exploration: oil from chalks, a modern miracle? *, 61*(7. (July)).

Sheng, James. (2010). Modern chemical enhanced oil recovery: theory and practice (pp. 73). Burlington, MA: Gulf Professional Pub.

Sylte, J. E., Thomas, L. K., Rhett, D. W., Bruning, D. D., & Nagel, N. B. (1999). *Water Induced Compaction in the Ekofisk Field*. Paper presented at the SPE Annual Technical Conference and Exhibition, Houston, Texas. http://www.onepetro.org/mslib/app/Preview.do?paperNumber=00056426&societyCode=SPE

Veen, Steffen Helgesen van der. (2012). *Water induced compaction of chalks with varying non-carbonate content : the effect of Mg2+ and pH of the injected brines*. Stavanger: S.H. van der Veen.

Wan, Richard, Alsaleh, Mustafa, & Labuz, Joe. (2011). *Bifurcations, Instabilities and Degradations in Geomaterials*. Berlin, Heidelberg: Springer Berlin Heidelberg.